

Bayesian Image Mediation Analysis

Yuliang Xu and Jian Kang*

Department of Biostatistics, University of Michigan

October 26, 2023

Abstract

Mediation analysis aims to separate the indirect effect through mediators from the direct effect of the exposure on the outcome. It is challenging to perform mediation analysis with neuroimaging data which involves high dimensionality, complex spatial correlations, sparse activation patterns and relatively low signal-to-noise ratio. To address these issues, we develop a new spatially varying coefficient structural equation model for Bayesian Image Mediation Analysis (BIMA). We define spatially varying mediation effects within the potential outcome framework, employing the soft-thresholded Gaussian process prior for functional parameters. We establish the posterior consistency for spatially varying mediation effects along with selection consistency on important regions that contribute to the mediation effects. We develop an efficient posterior computation algorithm scalable to analysis of large-scale imaging data. Through extensive simulations, we show that BIMA can improve the estimation accuracy and computational efficiency for high-dimensional mediation analysis over the existing methods. We apply BIMA to analyze the behavioral and fMRI data in the Adolescent Brain Cognitive Development (ABCD) study with a focus on inferring the mediation effects of the parental education level on the children's general cognitive ability that are mediated through the working memory brain activities.

Keywords: spatially varying mediation effects; Soft thresholded Gaussian process; Posterior consistency.

*To whom correspondence should be addressed: Jian Kang (jiankang@umich.edu)

1 Introduction

Mediation analysis is an important statistical tool that decomposes the total effects of an exposure or treatment variable on an outcome variable into direct effects and indirect effects through mediator variables (MacKinnon, 2012). Mediation analysis has been widely adopted to gain insights into mechanisms of exposure-outcome effects in many research areas including epidemiology, environmental science, genomics, and neuroimaging. Recent advances in neuroimaging have presented great opportunities and challenges for mediation analysis with large-scale complex neuroimaging data. In many neuroimaging studies, it is of great interest to identify important brain image mediators that mediate the effect of an exposure variable, such as age, social economic status, medical treatment, or substance use, to an outcome variable, such as the cognitive status, disease status.

Our work is motivated by the brain image mediation analysis in the Adolescent Brain Cognitive Development (ABCD) study, the largest long-term study of brain development and child health in the United States. Our objective is to investigate how parental education levels impact the children’s general cognitive ability that is mediated through brain function development measured by working memory task fMRI.

We consider voxel-level task fMRI contrast maps as the image mediators which pose several challenges for mediation analysis. First, the number of voxel-level image mediators can be up to 200,000 in a standard brain template, potentially requiring large computational resources for implementing the statistical algorithm. Second, brain image mediators exhibit complex correlation patterns such as the correlations among neighboring voxels and the correlation between brain regions with the same functions. Ignoring or inappropriately accounting for the correlation may introduce bias or lose statistical efficiency in estimating the mediation effects. Third, due to the low signal to noise ratio of brain imaging data, the voxel-level image mediators may have weak or zero effects on the outcome variable. The standard mediation analysis approach may suffer from low power and high false positive

rates when detecting active mediators.

Recent work on high dimensional mediation analysis provides different angles to tackle these challenges, with different statistical models tailored to specific application domains, such as penalized high dimensional survival analysis (Luo et al., 2020), DNA methylation markers (Zhang et al., 2016; Guo et al., 2022). For imaging applications, Lindquist (2012) first extended the mediation analysis framework into functional data analysis and proposed a model based on least-squares estimation and penalized regression, without considering correlation among individual level noises in the mediators. Built upon this work, Chén et al. (2018) proposed a method based on principle component analysis, where high dimensional correlated mediators are mapped to uncorrelated ones through orthogonal transformation. The orthogonal maps are sequentially estimated from maximizing the likelihood of the joint model on each direction of mediators separately. However, interpreting the estimated coefficients relies on untestable assumptions that mediators are randomly assigned to individuals, making the functional causal effect inseparable from the individual level noise.

Aside from the sequential mediator modeling idea, Zhao and Luo (2022) proposed a marginal mediator model with correlated error term, and defined a convex Pathway Lasso penalty to penalize the product term in the indirect effect, instead of penalizing each functional coefficient. The Pathway Lasso method demonstrated strong computation efficiency and accuracy compared to the sequential mediator model, but sparsity in the functional coefficients was not considered. Zhao et al. (2020) proposed another frequentist approach to high dimensional mediation problems, where sparse principle component analysis is used to map the correlated mediators onto a space of independent mediators, and penalized regression techniques such as the elastic net are employed in the outcome model to enforce sparsity in high dimensional mediators. Nath et al. (2023) used machine learning models to map a high dimensional imaging mediator to a single latent variable and treated this single latent variable as a mediator in the classical mediation triangle, sacrificing the interpretability of

mediation effects.

Focusing on the temporal mediation effects, [Zhao and Luo \(2019\)](#) proposed Granger mediation analysis, a novel framework for causal mediation analysis of multiple time series, inspired by an fMRI experiment. The framework combines causal mediation analysis and vector autoregressive (VAR) models to address challenges in time-series data, improving estimation bias and statistical power compared to existing approaches.

For Bayesian analysis of mediation effects, [Yuan and MacKinnon \(2009\)](#) presented a pioneering work in both single-level and multi-level models, demonstrating that Bayesian mediation analysis can improve estimation efficiency by incorporating prior knowledge. [Song et al. \(2020a\)](#) proposed Bayesian mixture models to account for a large set of correlated mediators with application to biomarker identification. In particular, to deal with the sparsity and correlation in a high dimensional parameter, a membership parameter was used to indicate whether the signal at a certain location is zero or not, and correlation structure is assumed for this membership parameter. In [Song et al. \(2020b\)](#) and [Song et al. \(2020c\)](#), different types of Bayesian mixture models were proposed with less focus on the correlation among different locations. In Section 5.1 we provide more details to these methods and compare them with our proposed method through simulation studies.

To the best of our knowledge, there is a lack of a Bayesian mediation analysis method for high-dimensional imaging data that can incorporate flexible spatial correlation structure, individual-level spatial noise, and sparsity in the functional coefficients. To fill this gap, we propose a new structural equation model with spatially varying coefficients and adopt the soft-thresholded Gaussian processes ([Kang et al., 2018](#), STGP) as priors for Bayesian Image Mediation Analysis (BIMA). Under the potential outcome framework, the proposed BIMA framework consists of two spatially varying coefficient models: a scalar-on-image regression model for the joint effect from the exposure and the image mediator on the outcome (the outcome model), and an image-on-scalar regression model for the effect of the exposure

on the image mediator (the mediator model). By assigning the STGP priors, we ensure large prior support for the piecewise smooth and sparse spatially varying coefficients in both models, based on which we formally define the spatially varying mediation effects under the potential outcome framework. To accommodate population heterogeneity in imaging data, we introduce spatially varying random effects for each individual in the mediator model, improving the efficiency of estimating the mediation effects. For posterior computation, we develop a modified Metropolis-adjusted Langevin algorithm (MALA) that boosts the computational efficiency via block updating and is scalable to high-dimensional imaging data analysis with many observations.

We perform rigorous theoretical analyses of BIMA. We establish the posterior consistency of all the spatially varying coefficients in the mediator and outcome models under the L_2 empirical norm, leading to the posterior consistency of the spatially varying mediation effects under the L_1 empirical norm. Different from the previous theoretical work on Bayesian scalar-on-image models (Kang et al., 2018), the image mediation analysis requires us to address the randomness of the functional mediator in the scalar-on-image outcome model while considering the mediator model as the generative model. Hence we proposed a new formulation for functional mediation where the mediator is treated as a random signed measure in the outcome model, and as a random function in the mediator model. This new formulation provides a coherent definition of the natural indirect effect with existing mediation literature while keeping the image mediator bounded in probability in the outcome model.

The rest of the article is structured as follows. In Section 2, we introduce the BIMA framework with definitions, models and prior specifications. In Section 3, we perform the theoretical analysis of the proposed methods, where we establish model identifiability and posterior consistency of the spatially varying mediation effects. Then, we develop the posterior computation algorithm in Section 4 and perform extensive simulations in Section 5.

Finally, we apply BIMA to the analysis of the fMRI and cognitive data in the Adolescent Brain Cognitive Development (ABCD) study in Section 6 and conclude the paper in Section 7.

2 Bayesian Image Mediation Analysis

2.1 General Notations

Let \mathbb{R}^d denote a d -dimensional Euclidean vector space. Let $\mathcal{S} \subset \mathbb{R}^d$ be a compact support. Let $N(\mu, \sigma^2)$ represent a normal distribution with mean μ and variance σ^2 . Let $L^2(\mathcal{S})$ be the space of square-integrable functions supported on \mathcal{S} . Let $\{s_1, \dots, s_p\}$ be a set of p fixed design points in \mathcal{S} . For any function $f(s)$ in $L^2(\mathcal{S})$, let $\|f\|_{q,p} = \left\{ p^{-1} \sum_{j=1}^p |f(s_j)|^q \right\}^{1/q}$ be the L_q empirical norm on the fixed grid with p voxels. For any vector $\mathbf{a} = (a_1, \dots, a_d)^\top \in \mathbb{R}^d$, let $\|\mathbf{a}\|_q = \left\{ \sum_{i=1}^d |a_i|^q \right\}^{1/q}$ be the L_q vector norm. For any functions $f, g \in L^2(\mathcal{S})$, define the inner product $\langle f, g \rangle := \int_{\mathcal{S}} f(s)g(s)\lambda(ds)$ where λ is the Lebesgue measure. The empirical inner product is defined as $\langle f, g \rangle_p := p^{-1} \sum_{j=1}^p f(s_j)g(s_j)$. Let $\mathcal{C}^\rho(\mathcal{S})$ be the order- ρ Hölder space on \mathcal{S} for a positive integer ρ . For a set \mathcal{B} , $\bar{\mathcal{B}}$ is used to denote the closure of the set, and $\partial\mathcal{B}$ denotes the boundary. Let $\mathcal{GP}(\nu, \kappa)$ denote a Gaussian Process with mean function $\nu(\cdot)$ and covariance matrix $\kappa(\cdot, \cdot)$.

2.2 Spatially-Varying Coefficient Structural Equation Models

Suppose the data consists of n individuals. For individual i ($i = 1, \dots, n$), let Y_i denote the outcome variable, X_i denote the exposure variable, $\mathbf{C}_i = (C_{i,1}, \dots, C_{i,q})^\top \in \mathbb{R}^q$ be a vector of q potential confounding variables. Suppose the imaging data are observed on a compact support \mathcal{S} . Let $\{\Delta s_1, \dots, \Delta s_p\}$ are a partition of \mathcal{S} , i.e., $\mathcal{S} = \bigcup_{j=1}^p \Delta s_j$ and $\Delta s_j \cap \Delta s_{j'} = \emptyset$. Let s_j be the center of the voxel Δs_j for $j = 1, \dots, p$. Let $\mathbf{M}_i = \{M_i(s_j), \dots, M_i(s_p)\}^\top$ be a vector of observed image intensities, where $M_i(s)$ represent the image intensity function at location $s \in \mathcal{S}$.

To perform image mediation analysis, we consider spatially varying coefficient structural

equation models which consist of scalar-on-image regression as the outcome model (1) and image-on-scalar regression as the mediator model (2). For $i = 1, \dots, n$, we assume

$$Y_i = \sum_{j=1}^p \beta(s_j) \mathcal{M}_i(\Delta s_j) + \gamma X_i + \boldsymbol{\xi}^\top \mathbf{C}_i + \epsilon_{Y,i}, \quad \epsilon_{Y,i} \stackrel{\text{iid}}{\sim} \text{N}(0, \sigma_Y^2), \quad (1)$$

$$M_i(s_j) = \alpha(s_j) X_i + \boldsymbol{\zeta}^\top(s_j) \mathbf{C}_i + \eta_i(s_j) + \epsilon_{M,i}(s_j), \quad \epsilon_{M,i}(s_j) \stackrel{\text{iid}}{\sim} \text{N}(0, \sigma_M^2) \quad (2)$$

where $\mathcal{M}_i(\Delta s) = \int_{\Delta s} M_i(s) \lambda(ds)$ is the total intensity measure over the small partition Δs and $\lambda(\cdot)$ is the Lebesgue measure. Throughout this paper, we assume that the Lebesgue measure on one partition $\lambda(\Delta s_j) = p^{-1}$ for any $j = 1, \dots, p$.

In the outcome model (1), $\beta(s)$ represents the spatially-varying effects of the image mediator on the outcome variable. The scalar coefficient γ is the direct effect of X_i on Y_i . The vector coefficient $\boldsymbol{\xi} \in \mathbb{R}^q$ represents the confounding effects. The random noises $\epsilon_{Y,i}$ are independent and follow a normal distribution with mean zero and variance σ_Y^2 .

In the mediator model (2), $\alpha(s)$ is the spatially-varying functional parameter of our interest. $\boldsymbol{\zeta}(s) = \{\zeta_1(s), \dots, \zeta_q(s)\}^\top$ is a vector of the coefficients for the confounders; $\eta_i(s)$ is the spatially-varying individual effect that capture the individual variations unexplained by the exposure variable X_i and the observed confounders \mathbf{C}_i ; and $\epsilon_{M,i}(s_j)$ is the spatially independent noise term across locations and subjects with constant variance σ_M^2 .

2.3 Connection to the Wiener process

When \mathcal{S} is one-dimensional, the finite summation $\sum_{j=1}^p \beta(s_j) \mathcal{M}_i(\Delta s_j)$ in model (1) is an approximation to the continuous integral $\int_{\mathcal{S}} \beta(s) \mathcal{M}_i(ds)$. In fact, when $\mathcal{S} = [0, 1] \in \mathbb{R}$, the continuous version of model (1) and (2) can be represented as

$$Y_i = \int_{\mathcal{S}} \beta(s) \mathcal{M}_i(ds) + \gamma X_i + \boldsymbol{\xi}^\top \mathbf{C}_i + \epsilon_{Y,i},$$

$$\mathcal{M}_i(ds) = \{\alpha(s) X_i + \boldsymbol{\zeta}^\top(s) \mathbf{C}_i + \eta_i(s)\} \lambda(ds) + \sigma_M dW_{i,M}(s), \quad (3)$$

where $\epsilon_{Y,i} \stackrel{\text{iid}}{\sim} N(0, \sigma_Y^2)$ and $W_{i,M}(s)$ is the Wiener process (Durrett, 2019).

In neuroimaging applications, we can only observe $M_i(s)$ on fixed grids $\{j = 1, \dots, p\}$, without loss of generality, we can approximate the values of $M_i(s)$, $\alpha(s)$, $\zeta(s)$ and $\eta_i(s)$ within each Δs_j by the functional values at its center s_j . Therefore the model (3) can be approximated by

$$\mathcal{M}_i(\Delta s_j) = \{\alpha(s_j)X_i + \zeta^\top(s_j)\mathbf{C}_i + \eta_i(s_j)\} \lambda(\Delta s_j) + \epsilon_{M,i}(\Delta s_j), \quad (4)$$

where $\epsilon_{M,i}(\Delta s_j) \sim N\{0, \sigma_M^2 \lambda(\Delta s_j)\}$. The advantage of using $\sum_{j=1}^p \beta(s_j) \mathcal{M}_i(\Delta s_j)$ in the scalar-on-image model (1) compared to other existing formulations (Kang et al., 2018; Lindquist, 2012) can be explained in two ways. First, the finite summation in (4) is a natural approximation to the inner-product on $L^2(\mathcal{S})$, hence in mediation analysis, as explained in the next section, we can naturally express the total indirect effect as $\sum_{j=1}^p \beta(s_j) \alpha(s_j) \lambda(\Delta s_j)$. Other formulations such as $\beta(s_j) M_i(s_j) / \sqrt{p}$ in Kang et al. (2018) do not have this property. Second, the variance of $\epsilon_{M,i}(\Delta s_j)$ is by design proportional to $\lambda(\Delta s_j)$ instead of $(\lambda(\Delta s_j))^2$. This plays a key role in constructing a test function when showing the posterior consistency in model (1), and ensures that we have enough variability in the design matrix in (1) to be able to estimate $\beta(s)$. In fact, the $M_i(s_j) / \sqrt{p}$ as used in Kang et al. (2018) also has the variance proportional to $1/p$, but they assume the mean part of $M_i(s)$ to be zero for all $s \in \mathcal{S}$, so that $\beta(s_j) \mathbb{E}\{M_i(s_j)\} / \sqrt{p}$ will not explode as $p \rightarrow \infty$, but this assumption is not practical in mediation problem. Lindquist (2012) also uses an inner product formulation, but they only assume that all the functional parameters can be represented by finitely many basis functions, and the number of basis does not increase with n or p , whereas in our case, we study all sparse, piece-wise smooth function in $L_2(\mathcal{S})$.

2.4 Causal Mediation Analysis

We define the main mediation parameter of interest first.

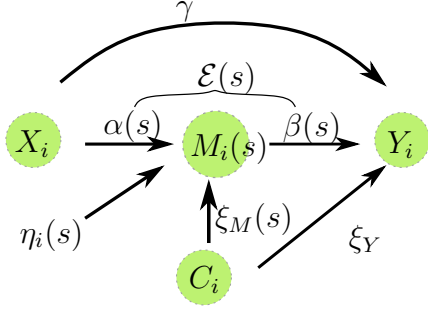


Figure 1: Graphical illustration of the structure of the proposed model

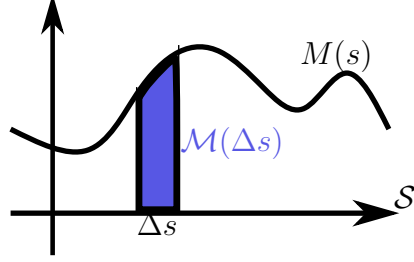


Figure 2: Illustration of the definitions of the intensity measure $\mathcal{M}(\Delta s)$ and the intensity function $M(s)$ in one-dimensional support \mathcal{S} .

Definition 1. Let $\mathcal{E}(s) = \alpha(s)\beta(s)$ be the *spatially-varying mediation effect (SVME) function*.

Under the causal inference framework (Rubin, 1974), for individual i , we define $Y_{i,(x,\mathbf{m})}$ as the potential outcome variable that would have been observed when the image mediator $\mathbf{M}_i = \mathbf{m}$ and the exposure variable $X_i = x$; and define $\mathbf{M}_{i,(x)}$ as the potential image mediator when the individual i receive exposure x . When the exposure variable X_i changes from x to x' , combining equations (1) and (4), we represent the natural indirect effect (NIE) and the natural direct effect (NDE) as follows:

$$\text{NIE}(x, x') = \mathbb{E} \left[Y_{i,\{x, \mathbf{M}_{i,(x)}\}} - Y_{i,\{x, \mathbf{M}_{i,(x')}\}} \mid \mathbf{C}_i \right] = \sum_{j=1}^p \beta(s_j) \alpha(s_j) \lambda(\Delta s_j) (x - x'), \quad (5)$$

$$= \sum_{j=1}^p \mathcal{E}(s_j) \lambda(\Delta s_j) (x - x') \quad (6)$$

$$\text{NDE}(x, x') = \mathbb{E} \left[Y_{i,\{x, \mathbf{M}_{i,(x')}\}} - Y_{i,\{x', \mathbf{M}_{i,(x')}\}} \mid \mathbf{C}_i \right] = \gamma(x - x'). \quad (7)$$

To ensure the above definitions are valid under the causal inference framework, we make the stable unit treatment value assumption (SUTVA) (Rubin, 1980) and the following modeling assumptions: for any i , x and \mathbf{m} , (1) $Y_{i,(x,\mathbf{m})} \perp X_i \mid \mathbf{C}_i$, (2) $Y_{i,(x,\mathbf{m})} \perp \mathbf{M}_i \mid \{\mathbf{C}_i, X_i\}$, (3) $\mathbf{M}_{i,(x)} \perp X_i \mid \mathbf{C}_i$, (4) $Y_{i,(x,\mathbf{m})} \perp \mathbf{M}_{i,(x')} \mid \mathbf{C}_i$. These assumptions ensure that: (i) NIE and NDE can be identified, and (ii) NIE and NDE can be estimated from observable

data. See [VanderWeele and Vansteelandt \(2014\)](#) for the detailed interpretation of the above assumptions.

In image mediation analysis, we are interested in which locations contribute to the NIE or the mediation effects. From (6), it is straightforward to see that $\mathcal{E}(s_j)$ represents the contribution of location s_j to the NIE(x, x') for any $x \neq x'$, which is the motivation of Definition 1. For any location $s \in \mathcal{S}$, $\mathcal{E}(s)$ characterizes the impact of the location s on the NIE. Both $\mathcal{E}(s)$ and $p^{-1} \sum_{j=1}^p \mathcal{E}(s_j)$ are the parameters of our main interest. It is generally believed that not all brain locations contribute to the mediation effects, and $\mathcal{E}(s)$ is naturally a sparse function when $\alpha(s)$ and $\beta(s)$ are both sparse.

2.5 Prior Specifications

To model the sparsity and the spatial smoothness in the spatially varying mediation effects $\mathcal{E}(s)$, we adopt the soft-thresholded Gaussian process (STGP) proposed in [Kang et al. \(2018\)](#) for $\alpha(s)$ and $\beta(s)$, separately. For the individual effects $\eta_i(s)$ and confounding effects $\zeta_k(s)$, we assign the regular Gaussian process priors. Let $T_\nu : \mathbb{R} \mapsto \mathbb{R}$ be a soft-thresholded operator defined as $T_\nu(x) := \{x - \text{sgn}(x)\nu\}I(|x| > \nu)$ for any $\nu \geq 0$.

Definition 2 ([Kang et al. \(2018\)](#)). *Let $\tilde{f}(s)$ be a Gaussian process (GP) with mean zero and the covariance kernel κ_f , denoted as $\tilde{f} \sim \mathcal{GP}(0, \kappa_f)$. For any $\nu \geq 0$, set $f(s) = T_\nu\{\tilde{f}(s)\}$. Then $f(s)$ is a STGP with covariance kernel κ_f and threshold parameter ν , denoted as $f \sim \text{STGP}(\nu_f, \kappa_f)$.*

In summary, we have the following prior specifications,

$$\beta \sim \text{STGP}(\nu_\beta, \sigma_\beta^2 \kappa), \quad \alpha \sim \text{STGP}(\nu_\alpha, \sigma_\alpha^2 \kappa), \quad \zeta_k \sim \mathcal{GP}(0, \sigma_\zeta^2 \kappa), \quad \eta_i \sim \mathcal{GP}(0, \sigma_\eta^2 \kappa), \quad (8)$$

for $i = 1, \dots, n$ and $k = 1, \dots, q$. As explained in Section 3.2 in [Kang et al. \(2018\)](#), given a positive threshold value $\nu > 0$, STGP is flexible to fit a wide range of sparsity levels. The specific values for the thresholding parameters ν_α and ν_β in practice are chosen within a

reasonable range according to the effect size of α and β .

The choice of κ , the kernel function for the latent Gaussian process, controls the smoothness of the functional parameters. For the rest of the parameters, the normal priors with mean zero are assigned for $\gamma, \boldsymbol{\xi}$, the inverse-gamma priors are assigned for the variance parameters $\sigma_Y^2, \sigma_M^2, \sigma_\beta^2, \sigma_\alpha^2$ and σ_η^2 .

3 Theoretical Properties

This section aims to establish the posterior consistency for spatially varying mediation effects $\mathcal{E}(s)$ under the empirical L_1 norm. To achieve this goal, we first show the posterior consistency for $\beta(s)$ in the outcome model (1) and $\alpha(s)$ in the mediator model (2), respectively. All the derivations and proofs are provided in the Supplementary Material.

3.1 Notations and Assumptions

To perform the theoretical analysis, we introduce additional notation. Let $\mathbf{Y} = (Y_1, \dots, Y_n) \in \mathbb{R}^n$, $\mathbf{X} = (X_1, \dots, X_n)^\top \in \mathbb{R}^n$, $\mathbf{M} = (\mathbf{M}_1, \dots, \mathbf{M}_n)^\top \in \mathbb{R}^{n \times p}$ and $\mathbf{C} = (\mathbf{C}_1, \dots, \mathbf{C}_n)^\top \in \mathbb{R}^{n \times q}$. Let $\alpha_0(s), \beta_0(s), \eta_{i,0}(s)$ and $\zeta_0(s)$ represent the corresponding true spatially varying coefficients in the BIMA models (1) and (2) that generate the observed data \mathbf{Y} and \mathbf{M} given \mathbf{X} and \mathbf{C} . Let $\mathcal{E}_0(s) = \alpha_0(s)\beta_0(s)$ represent the true spatially varying mediation effects. We assume that all those true spatially varying coefficients are square-integrable in $L^2(\mathcal{S})$. For matrix A , $\det(A)$ denotes the determinant of A , $\sigma_{\min}(A), \sigma_{\max}(A)$ denote the smallest and the largest singular value of A respectively.

Next, we define a functional space for the sparse and piecewise smooth spatially varying coefficients.

Definition 3 (Sparse functional space). *Define the sparse functional space $\Theta^{SP} = \{f(s) : s \in \mathcal{S}\}$ as the collection of spatially-varying coefficient functions that satisfy the three conditions.*

a) (Continuous) $f(s)$ is a continuous function on \mathcal{S} ; b) (Sparse) Assume there exist two disjoint nonempty open sets \mathcal{R}_{-1} and \mathcal{R}_1 , and $\partial\mathcal{R}_{-1} \cap \partial\mathcal{R}_1 = \emptyset$ such that $\forall s \in \mathcal{R}_1, f(s) > 0$;

$\forall s \in \mathcal{R}_{-1}, f(s) < 0$. $\mathcal{R}_0 = \mathcal{S} - (\mathcal{R}_1 \cup \mathcal{R}_{-1})$, and assume \mathcal{R}_0 has nonempty interior; and c) (Piecewise smooth) For any $s \in \bar{\mathcal{R}}_1 \cup \bar{\mathcal{R}}_{-1}$, $f(s) \in \mathcal{C}^\rho(\bar{\mathcal{R}}_1 \cup \bar{\mathcal{R}}_{-1})$, $\rho \geq 1$.

This definition has been adopted for specifying the true parameter space of scalar-on-image regression, see Definition 2 in Kang et al. (2018). In BIMA, $\alpha(s)$ and $\beta(s)$ are assumed to be in the sparse functional space in Definition 3, and later in the proof of Theorem 3, we will show that $\mathcal{E}(s)$ as defined in Definition 1 also belongs to the sparse functional space in Definition 3 when both $\alpha(s)$ and $\beta(s)$ are in this sparse functional space. In brain imaging application, we also consider region parcellation based on the anatomic structure of the human brain. When we allow a partition of R regions in the support \mathcal{S} , $\mathcal{S} = \cup_{r=1}^R \mathcal{S}_r$, we make the additional assumption that there is no piece-wise smooth area across different regions for α and β , which means that the nonzero areas in α and β only exist within each region \mathcal{S}_r , and not across regions or on the region boundaries. Hence, α and β are still continuous functions on \mathcal{S} .

Next, we will introduce the parameter space for each of the functional parameters in model (1)-(2).

Definition 4 (Parameter space). Let $\Theta_\alpha, \Theta_\beta, \Theta_\eta, \Theta_\zeta$ be the parameter space for $\alpha, \beta, \{\eta_i\}_{i=1}^n, \{\zeta_k\}_{k=1}^q$ respectively, and they are all subsets of the square-integrable space $L^2(\mathcal{S})$. Let $\{\psi_l(s)\}_{l=1}^\infty$ be a set of basis of $L^2(\mathcal{S})$, we specify the following constraints for each parameter space: (a) $\Theta_\alpha \subset \Theta^{SP}$; (b) $\Theta_\beta \subset \Theta^{SP}$, and for any $\beta \in \Theta_\beta$, define $\theta_{\beta,l} = \int_{\mathcal{S}} \beta(s)\psi_l(s)\lambda(ds)$, there exists $L_n = n^{\nu_1}$ where $\nu_1 \in (0, 1)$ and $\nu_2 > 0$ such that $\sum_{l=L_n}^\infty \theta_{\beta,l}^2 \leq L_n^{-\nu_2}$; (c) $\Theta_\eta, \Theta_\zeta \subset C^\rho(\mathcal{S})$; (d) There exists a constant $K > 0$ such that for any f, g in $\Theta_\alpha, \Theta_\beta, \Theta_\eta, \Theta_\zeta$ and $\{\psi_l(s)\}_{l=1}^\infty$, the fixed grid approximation error $|\int_{\mathcal{S}} f(s)g(s)\lambda(ds) - p^{-1} \sum_{j=1}^p f(s_j)g(s_j)| \leq Kp^{-2/d}$.

Remark. In the case of region partition $\mathcal{S} = \cup_{r=1}^R \mathcal{S}_r$, we can construct the basis based on each region. Let $\{\psi_{l,r}(s)\}_{l=1}^\infty$ be the basis of $L^2(\mathcal{S}_r)$, and construct $\psi_l(s) = \sum_{r=1}^R \psi_{l,r}(s)I(s \in \mathcal{S}_r)$. The basis decomposition for $f(s) \in L^2(\mathcal{S})$ can be written as $\theta_{f,l} = \int_{\mathcal{S}} \psi_l(s)f(s)\lambda(ds) =$

$\sum_{r=1}^R \int_{\mathcal{S}_r} \psi_l(s) f(s) \lambda(ds) = \sum_{r=1}^R \theta_{f,r,l}$. The decay rate condition in Definition 4 stays the same for $\theta_{f,l}$ because of the finite summation.

In Definition 4, (a)-(c) define the smoothness and sparse feature of the parameter space, where $\alpha(s)$, $\beta(s)$ are assumed to be piecewise-smooth, sparse and continuous functions, and the individual effect $\eta_i(s)$ and the confounding effects $\zeta_k(s)$ in model (2) are only required to be smooth but not necessarily sparse. Definition 4(d) sets an upper bound for the fixed grid approximation error. Assumption 1 below specifies the smoothness of the underlying Gaussian processes and the rate of p as $n \rightarrow \infty$.

Assumption 1. *Given the dimension d of \mathcal{S} and a constant τ satisfying $d > 1 + 1/\tau$, $\tau \geq 1$, assume that a) (Smooth Kernel) for each s , the kernel function $\kappa(s, \cdot)$ introduced in the priors (8) has continuous partial derivatives up to order $2\rho + 2$ for some positive integer ρ , i.e. $\kappa(s, \cdot) \in \mathcal{C}^{2\rho+2}(\mathcal{S})$, and $d + 3/(2\tau) < \rho$; b) (Dimension Limits) $p \geq O(n^{\tau d})$.*

The Assumption 1(a) is the standard condition (Ghosal and Roy, 2006) to ensure the sufficient smoothness of the latent Gaussian processes $\tilde{\beta}(s)$, $\tilde{\alpha}(s)$, $\zeta_k(s)$ and $\eta_i(s)$. The Assumption 1(b) is to specify the order of the number of voxels as the sample size increases, implying that our method can handle high resolution images.

As the mediator model (2) involves spatially varying coefficients $\eta_i(s)$ as individual effect parameters, the model identifiability is not trivial and requires some mild conditions on the observations of exposure variables and confounding factors.

Assumption 2. *(a) Each element in (\mathbf{X}, \mathbf{C}) has a finite fourth moment with sub-Gaussian tails, and $\sigma_{\min}\{(\mathbf{X}, \mathbf{C})\} > \sqrt{n}$ almost surely; (b) Conditioning on (\mathbf{X}, \mathbf{C}) , there exists a matrix $\mathbf{W} = (W_{i,k}) \in \mathbb{R}^{n \times (q+1)}$ such that $\det\{\mathbf{W}^\top(\mathbf{X}, \mathbf{C})\} \neq 0$; and (c) there exists a constant vector $\mathbf{b} = (b_1, \dots, b_q)^\top$ such that for any $s \in \mathcal{S}$ and $k = 1, \dots, q + 1$, $\sum_{i=1}^n W_{i,k} \eta_i(s) = b_k$.*

Assumption 2(a) is a reasonable assumption in linear regression with the design matrix (\mathbf{X}, \mathbf{C}) (Armagan et al., 2013). For (b) and (c), one example that can satisfy the above

assumption is to set $b = 0 \in \mathbb{R}^{q+1}$, $\mathbf{W} = (\mathbf{X}, \mathbf{C})$, and if we express $\eta_i(s) = \sum_{l=1}^{\infty} \theta_{\eta,i,l} \psi_l(s)$ as infinite sums of basis in the Hilbert space, then each $(\theta_{\eta,i,l})_{l=1}^n \in \mathbb{R}^n$ is generated from a subspace orthogonal to $\text{span}\{\mathbf{X}, \mathbf{C}_1, \dots, \mathbf{C}_q\}$. We enforce this assumption in the sampling algorithm by updating $(\theta_{\eta,i,l})_{l=1}^n$ from a constrained multivariate normal distribution.

With Assumption 2, we can establish the model identifiability in (2) and show that if the spatially varying coefficients are different from the true value, the mean function of $M_i(s)$, denoted as $\mu_{M,i}(s) := \alpha(s)X_i + \boldsymbol{\zeta}^\top(s)\mathbf{C}_i + \eta_i(s)$, will also be deviated from the true mean function $\mu_{M,i,0}(s) := \alpha_0(s)X_i + \boldsymbol{\zeta}_0^\top(s)\mathbf{C}_i + \eta_{i,0}(s)$.

Let $\Theta_M = \Theta_\alpha \times \Theta_\zeta \times (\prod_i \Theta_{\eta,i})$ be the joint parameter space for all parameters in the mean function $\mu_{M,i}(s)$. For any $\epsilon > 0$ and some constant $c_0 > 0$, define the following two subsets of Θ_M as

$$\begin{aligned} \mathcal{U}_M^c &= \left\{ \Theta_M : \|\alpha - \alpha_0\|_{2,p}^2 + \sum_{k=1}^q \|\zeta_k - \zeta_{k,0}\|_p^2 + \frac{1}{n} \sum_{i=1}^n \|\eta_i - \eta_{i,0}\|_{2,p}^2 > \epsilon^2 \right\} \\ \mathcal{U}_{M,\mu}^c &= \left\{ \Theta_M : \frac{1}{n} \sum_{i=1}^n \|\mu_{M,i} - \mu_{M,i,0}\|_{2,p}^2 > c_0 \epsilon^2 \right\} \end{aligned}$$

Proposition 1. *Under Assumptions 2, (a) the mediator model (2) is identifiable; and (b) $\mathcal{U}_M^c \subset \mathcal{U}_{M,\mu}^c$ almost surely with respect to (\mathbf{X}, \mathbf{C}) .*

3.2 Posterior consistency

First, we show joint posterior consistency of all the spatially varying coefficients in the mediator model (2) as the number of images $n \rightarrow \infty$ and the number of voxels $p \rightarrow \infty$.

The following empirical L_2 norm consistency result is proved by verifying conditions in Theorem A.1 in Choudhuri et al. (2004). For the proof of existence of test, we borrow techniques from Proposition 11 in van der Vaart and van Zanten (2011).

Theorem 1. *Suppose Assumptions 1-2 hold in the mediator model (2). For any $\epsilon > 0$, as $n \rightarrow \infty$, we have $\Pi(\mathcal{U}_M^c \mid \mathbf{M}, \mathbf{X}, \mathbf{C}) \rightarrow 0$ in P_0^n -probability. This further implies that*

$\Pi(\|\alpha - \alpha_0\|_{2,p} > \epsilon \mid \mathbf{M}, \mathbf{X}, \mathbf{C}) \rightarrow 0$ and $\Pi(n^{-1} \sum_{i=1}^n \|\eta_i - \eta_{i,0}\|_{2,p}^2 > \epsilon^2 \mid \mathbf{M}, \mathbf{X}, \mathbf{C}) \rightarrow 0$ in P_0^n -probability.

Next, we give the L_2 consistency result on $\beta(s)$ with the following notations and assumptions.

For any $f \in L^2(\mathcal{S})$, given the basis $\{\psi_l(s)\}_{l=1}^\infty$ in Definition 4, $f(s) = \sum_{l=1}^\infty \theta_{f,l} \psi_l(s)$, where $\sum_{l=1}^\infty \theta_{f,l}^2 < \infty$. Let $r_L(s) = \sum_{l=L}^\infty \theta_{f,l} \psi_l(s)$ be the remainder term after choosing a cutoff L as the finite sum approximation. Note that the remainder term $\int_{\mathcal{S}} r_L(x)^2 \lambda(ds) = \sum_{l=L}^\infty \theta_{f,l}^2 \rightarrow 0$ as $L \rightarrow \infty$ (Appendix E in Ghosal and van der Vaart (2017)). We employ the basis expression to show the posterior consistency in model (1), especially for studying the role of $\mathcal{M}_i(\Delta s_j)$.

Denote $\tilde{\gamma} = (\gamma, \boldsymbol{\xi}^\top)^\top \in \mathbb{R}^{q+1}$, $\tilde{\mathbf{X}}_i = (X_i, \mathbf{C}_i^\top)^\top \in \mathbb{R}^{q+1}$. Let $\beta(s) = \sum_{l=1}^\infty \theta_{\beta,l} \psi_l(s_j)$. Let $\tilde{\mathcal{M}}_{i,l} = \sum_{j=1}^p \psi_l(s_j) \mathcal{M}_i(\Delta s_j)$, and define the $n \times L_n$ matrix $\tilde{\mathcal{M}}_n := (\tilde{\mathcal{M}}_{i,l})_{i=1,\dots,n,l=1,\dots,L_n}$. Further, denote $\tilde{\mathbf{W}}_n = (\tilde{\mathcal{M}}_n, \tilde{\mathbf{X}}) \in \mathbb{R}^{n \times (L_n + 1 + q)}$ as the design matrix.

We state the following assumption for constructing the consistency test in Theorem 2.

Assumption 3. *The least singular value of $\tilde{\mathbf{W}}_n$ satisfies $0 < c_{\min} < \liminf_{n \rightarrow \infty} \sigma_{\min}(\tilde{\mathbf{W}}_n) / \sqrt{n}$ with probability $1 - \exp(-\tilde{c}n)$ for some constant $\tilde{c}, c_{\min} > 0$.*

A similar assumption has been made in Armagan et al. (2013). One extreme example that satisfies Assumption 3 is when $\tilde{\mathbf{W}}_n$ has mean-zero i.i.d. subgaussian entries. We will also give an example in the Supplementary Material B that satisfies Assumption 3 and follows the generative model (2) under some conditions.

Remark. Assumption 3 demonstrates the variability in the design matrix $\tilde{\mathbf{W}}_n$: the posterior consistency of $\beta(s)$ can only be guaranteed when the variability of the design matrix is sufficiently large, implying that the level of complexity of the functional parameter $\beta(s)$ we can possibly estimate is determined by the complexity of the input imaging data.

Theorem 2. *Suppose Assumptions 1 - 3 hold in the outcome model (1) and the priors on $\tilde{\gamma}$ satisfy that $\Pi(\|\tilde{\gamma} - \tilde{\gamma}_0\|_2^2 < \epsilon) > 0$ for any $\epsilon > 0$. Then for any $\epsilon > 0$, we have, as*

$n \rightarrow \infty$, $\Pi(\|\beta - \beta_0\|_{2,p} + \|\tilde{\gamma} - \tilde{\gamma}_0\|_2 > \epsilon \mid \mathbf{Y}, \mathbf{M}, \mathbf{X}, \mathbf{C}) \rightarrow 0$ in P_0^n -probability. This implies that $\Pi(\|\beta - \beta_0\|_{2,p} > \epsilon \mid \mathbf{Y}, \mathbf{M}, \mathbf{X}, \mathbf{C}) \rightarrow 0$ in P_0^n -probability.

In the proof of Theorem 2, especially in constructing the test for $H_0 : \beta(s) = \beta_0(s)$ v.s. $H_1 : \|\beta - \beta_0\|_{2,p} > \epsilon$ through the basis approximation of $\beta(s)$, verifying conditions in the Supplementary Material for $M_i(s)$ in model (2) provides insight into the relationship between models (1) and (2): sufficient variability in $M_i(s)$ ensures posterior consistency of $\beta(s)$.

Theorem 3. (*Posterior consistency of SVME*) Under Assumptions 1 - 3, for any $\epsilon > 0$, as $n \rightarrow \infty$, $\Pi(\|\mathcal{E} - \mathcal{E}_0\|_{1,p} < \epsilon \mid \mathbf{Y}, \mathbf{M}, \mathbf{X}, \mathbf{C}) \rightarrow 1$ in P_0^n -probability.

This theorem implies that the posterior distribution of SVME concentrates on an arbitrarily small neighborhood of its true value with probability tending to one when the sample size goes to infinity. Here the sample size refers to the number of images n . By Assumption 1, in this case, the number of voxels p also goes to infinity. This theorem also implies the consistency of estimating NIE using posterior inference by BIMA in the following corollary.

Corollary 1. (*Posterior consistency of NIE*) For any $\epsilon > 0$, as $n \rightarrow \infty$,

$$\Pi\left(p^{-1} \left| \sum_{j=1}^p \mathcal{E}(s_j) - \sum_{j=1}^p \mathcal{E}_0(s_j) \right| < \epsilon \mid \mathbf{Y}, \mathbf{M}, \mathbf{X}, \mathbf{C}\right) \rightarrow 1$$

in P_0^n -probability.

From Theorem 3, we can further establish the posterior sign consistency of SVME. Consider a minimum effect size $\delta > 0$, define $\mathcal{R}_\delta^+ = \{s : \mathcal{E}_0(s) > \delta\}$ and $\mathcal{R}_\delta^- = \{s : \mathcal{E}_0(s) < -\delta\}$, which represent the true positive SVME region and the true negative SVME region respectively. Let $\mathcal{R}_0 = \{s : \mathcal{E}_0(s) = 0\}$ represent a region of which the true SVME is zero.

Corollary 2. (*Posterior sign consistency of SVME*) For any $\delta > 0$, let $\mathcal{R}_\delta = \mathcal{R}_\delta^+ \cup \mathcal{R}_\delta^- \cup \mathcal{R}_0$, Then as $n \rightarrow \infty$, $\Pi[\text{sign}\{\mathcal{E}(s)\} = \text{sign}\{\mathcal{E}_0(s)\}, \forall s \in \mathcal{R}_\delta \mid \mathbf{Y}, \mathbf{M}, \mathbf{X}, \mathbf{C}] \rightarrow 1$ in P_0^n -probability, where $\text{sign}(x) = 1$ if $x > 0$, $\text{sign}(x) = -1$ if $x < 0$ and $\text{sign}(0) = 0$.

This corollary ensures that with a large posterior probability BIMA can identify the important regions with significant positive and negative SVMs that contributes the NIE.

4 Posterior Computation

The posterior computation for BIMA is challenging due to the complexity of the non-parametric inference, the high-dimensional parameter space and the non-conjugate prior specifications for the spatially-varying coefficients in the model. To address these challenges, we next construct an equivalent model representation.

4.1 Model representation and approximation

We approximate the STGPs and GPs using a basis expansion approach. By Mercer’s theorem (Williams and Rasmussen, 2006), the correlation kernel function in (8) can be decomposed by infinite series of orthonormal basis functions $\kappa(s, s') = \sum_{l=1}^{\infty} \lambda_l \psi_l(s) \psi_l(s')$, and the corresponding GP $g(s) \sim \mathcal{GP}(0, \sigma_g^2 \kappa)$ can be expressed as $g(s) = \sum_{l=1}^{\infty} \theta_{g,l} \psi_l(s)$ where $\theta_{g,l} \stackrel{\text{ind}}{\sim} N(0, \lambda_l \sigma_g^2)$.

In our implementation, we allow region partition to speed up the computation, and assume a region-independence prior kernel structure for the spatially varying parameters $\beta, \alpha, \zeta_k, \eta_i$. In real data analysis, the brain anatomic region parcellation defines the region partition. Assume there are $r = 1, \dots, R$ regions that form a partition of the support \mathcal{S} , denoted as $\mathcal{S}_1, \dots, \mathcal{S}_R$. The kernel function $\kappa(s_j, s_k) = 0$ for any $s_j \in \mathcal{S}_r, s_k \in \mathcal{S}_{r'}, r \neq r'$, and the prior covariance matrix on the fixed grid has a block diagonal structure. For the whole brain analysis as one region, one can choose $R = 1$.

For the r -th region, let p_r be the number of voxels in \mathcal{S}_r , $Q_r = (\psi_l(s_{r,j}))_{l=1, j=1}^{L_r, p_r} \in \mathbb{R}^{L_r \times p_r}$ be the matrix with the (l, j) -th component $\psi_l(s_{r,j})$, $\{s_{r,j}\}_{j=1}^{p_r}$ forms the fixed grid in \mathcal{S}_r . Because of the basis approximation with cutoff L_r , Q_r is not necessarily an orthonormal matrix, hence we use QR decomposition to get an approximated orthonormal Q_r , i.e. $Q_r^T Q_r = I_{L_r}$, where I_{L_r} is the identity matrix. With the region partition, the GP priors on the r -th region can

be approximated as $g_r = (g(s_{r,1}), \dots, g(s_{r,p_r}))^T \approx Q_r \boldsymbol{\theta}_{g,r}$, where $\boldsymbol{\theta}_{g,r} \sim \mathcal{N}(0, \sigma_g^2 D_r)$, D_r is a diagonal matrix with eigen-values $(\lambda_{r,1}, \dots, \lambda_{r,L_r})^T \in \mathbb{R}^{L_r}$.

After truncating the expansion at sufficiently large $\{L_r\}_{r=1}^L$, STGPs and GPs in the prior specifications (8), which all share the same kernel, can be approximated by

$$\begin{aligned} \beta_r &= T_\nu(\tilde{\beta}_r) \approx T_\nu(Q_r \boldsymbol{\theta}_{\tilde{\beta},r}), & \alpha_r &= T_\nu(\tilde{\alpha}_r) \approx T_\nu(Q_r \boldsymbol{\theta}_{\tilde{\alpha},r}), \\ \zeta_{k,r} &\approx Q_r \boldsymbol{\theta}_{\zeta,k,r}, & \eta_{i,r} &\approx Q_r \boldsymbol{\theta}_{\eta,i,r}, \end{aligned}$$

where the corresponding basis coefficients follow independent normal priors:

$$\boldsymbol{\theta}_{\tilde{\beta},r} \sim N_{L_r}(0, \sigma_{\tilde{\beta}}^2 D_r), \quad \boldsymbol{\theta}_{\tilde{\alpha},r} \sim N_{L_r}(0, \sigma_{\tilde{\alpha}}^2 D_r), \quad \boldsymbol{\theta}_{\zeta,k,r} \sim N_{L_r}(0, \sigma_{\zeta}^2 D_r), \quad \boldsymbol{\theta}_{\eta,i,r} \sim N_{L_r}(0, \sigma_{\eta}^2 D_r).$$

We discuss the details for choosing L_r in Section 4.2. Denote $\mathcal{M}_i(\mathcal{S}_r) = (\mathcal{M}_i(\Delta s_{r,j}))_{j=1}^{p_r} \in \mathbb{R}^{p_r}$, $M_i(\mathcal{S}_r) = (M_i(s_{r,j}))_{j=1}^{p_r} \in \mathbb{R}^{p_r}$, Then the BIMA model can be approximated as follows.

$$\begin{aligned} Y_i &= \sum_{r=1}^R T_\nu(Q_r \boldsymbol{\theta}_{\tilde{\beta},r}) \mathcal{M}_i(\mathcal{S}_r) + \gamma X_i + \boldsymbol{\zeta}_Y^T \mathbf{C}_i + \epsilon_{Y,i}, \\ M_i(\mathcal{S}_r) &= T_\nu(Q_r \boldsymbol{\theta}_{\tilde{\alpha},r}) X_i + \sum_{k=1}^q Q_r \boldsymbol{\theta}_{\zeta,k,r} C_{i,k} + Q_r \boldsymbol{\theta}_{\eta,i,r} + \epsilon_{M_r,i} \end{aligned}$$

where $\epsilon_{Y,i} \sim N(0, \sigma_Y^2)$ and $\epsilon_{M_r,i} \sim N_{p_r}(0, \sigma_M^2 I_{p_r})$. From the above model representation, both $\boldsymbol{\theta}_{\zeta,k,r}$ and $\boldsymbol{\theta}_{\eta,i,r}$ have conjugate posteriors, but T_ν is not a linear function, and $\boldsymbol{\theta}_{\tilde{\beta},r}$ and $\boldsymbol{\theta}_{\tilde{\alpha},r}$ do not have conjugate posteriors. To overcome this, the Metropolis-adjusted Langevin algorithm (MALA) is used to sample $\boldsymbol{\theta}_{\tilde{\beta},r}$ and $\boldsymbol{\theta}_{\tilde{\alpha},r}$. However, the first-order derivative of the soft-thresholded function $T_\nu(x)$ does not exist at the two change points $x = \pm\nu$. To approximate the first-order derivative, either the derivative of a smooth approximation function or a piece-wise function $d\hat{T}_\nu(x) = I(|x| \geq \nu)$ works in our case. The later one $d\hat{T}_\nu(x) = I(|x| \geq \nu)$ provides better computational efficiency, and is implemented in our algorithm.

4.2 Covariance kernel specifications and estimation

We can choose different covariance kernels for the GPs in models (1) and (2). Given the covariance kernel function $\kappa(\cdot, \cdot)$, to obtain the coefficients λ_l and the basis functions $\psi_l(s)$, Sections 4.3.1 and 4.3.2 in Williams and Rasmussen (2006) provide the analytic solution for squared exponential kernel, and an approximation method for other kernel functions with no analytic solutions. In practice when $\psi_l(s)$ has no analytical solutions, such as the Matérn kernel, we use eigen decomposition on the covariance matrix, and take the first L eigenvalues as the approximated λ_l , the first L eigenvectors as the approximated $\psi_l(s)$, then apply QR decomposition on the approximated basis functions to obtain orthonormal basis. The limitation of this method is that the covariance matrix is difficult to compute in high dimensions due to precision issues. Hence in high dimensions we split the entire space \mathcal{S} into smaller regions, and compute the basis functions on each region independently. This also aligns with the imaging application with the whole brain atlas. Another benefit is that by splitting the whole parameter space into smaller regions, the sampling space gets smaller and it becomes easier to accept the proposed vector $\beta(s)$ on each region with much less directions to explore. In practice, to choose the number of basis functions L_r for region r with p_r voxels, we first compute the covariance matrix in $\mathbb{R}^{p_r \times p_r}$ with appropriately tuned covariance parameters, get the eigen-value of such covariance matrix, and choose the cutoff such that the summation $\sum_{l=1}^{L_r} \lambda_l$ is over 90% of $\sum_{l=1}^{p_r} \lambda_l$, i.e. the eigenvalues before cutoff account for over 90% of the total eigenvalues. We provide the detailed sensitivity analysis on choosing the covariance parameters in the Supplementary Material.

4.3 The MCMC algorithm

We develop an efficient Markov chain Monte Carlo (MCMC) algorithm for posterior computation. To update parameters $\{\boldsymbol{\theta}_{\beta,r}, \boldsymbol{\theta}_{\alpha,r}\}_{r=1}^R$, we adopt the Metropolis-adjusted Langevin algorithm (MALA). The step size is tuned during the burn-in period to ensure an acceptance rate between 0.2 and 0.4. The target acceptance rate for each region is set to be proportional

to the inverse of the number of basis functions in that region, in order to produce a relatively large effective sample size of the MCMC sample.

To incorporate the block structure with MALA, in each iteration, the proposal $\boldsymbol{\theta}_{\tilde{\beta},r}$ or $\boldsymbol{\theta}_{\tilde{\alpha},r}$ for region \mathcal{S}_r is based on the target posterior density conditional on $\boldsymbol{\theta}_{\tilde{\beta},r'}$ or $\boldsymbol{\theta}_{\tilde{\alpha},r'}$ supported on all other regions where $r' \neq r$. The acceptance ratio is also computed region by region.

MALA has a considerable computational cost especially in high dimensional sampling, where the step size has to be very small to have an acceptance rate reasonably greater than 0. It is important to have a good initial value. To obtain the initial values, we consider a working model with the spatially varying coefficients $\beta(s)$ and $\alpha(s)$ following GP instead of STGP. With the basis expansion approach, we can straightforwardly use Gibbs sampling to obtain the approximated posterior samples of $\beta(s)$ and $\alpha(s)$ of the working model. The posterior mean values of $\beta(s)$ and $\alpha(s)$ estimated from the working model can be used to specify the initial value of the basis coefficients in the MALA algorithm. More detailed discussion on choosing the initial value can be found in Supplementary Material Section S4.

To impose identifiability Assumption 2, the posterior of $\theta_{\eta,i,l}$ is sampled from a constrained multivariate normal distribution, with the constraint $\tilde{\mathbf{X}}^T \boldsymbol{\theta}_{\eta,l} = \mathbf{0}$ where $\boldsymbol{\theta}_{\eta,l} = (\theta_{\eta,1,l}, \dots, \theta_{\eta,n,l})^T$. The algorithm for sampling multivariate normal distribution constrained on a hyperplane follows Algorithm 1 in (Cong et al., 2017).

For the rest of the parameters, with available conjugate full conditional posteriors, we use Gibbs sampling to update. The algorithm is implemented in Rcpp (Eddelbuettel and François, 2011) with RcppArmadillo (Eddelbuettel and Sanderson, 2014). The implementation is wrapped as an R package BIMA. ¹

5 Simulations

To demonstrate the performance of BIMA, two sets of simulation studies are analyzed. In the first simulation study, we compare the performance with other existing Bayesian me-

¹Available on Github <https://github.com/yuliangxu/BIMA>

diation methods in a low dimensional setting with relative small sample sizes, since some competing methods cannot handle high-dimensional settings efficiently. In the second simulation study, we vary the sample size, noise variance, and image patterns, and conduct a sensitivity analysis on the performance of our method under different settings with different prior specifications.

5.1 Comparison with existing methods

To make fully Bayesian inferences in mediation model, there exist a number of methods utilizing threshold priors and mixture models to impose sparsity and model correlation. In this section, we compare BIMA with two recently proposed Bayesian methods: product threshold Gaussian prior (PTG) and Correlated Selection Model (CorS).

Product Threshold Gaussian prior (PTG) (Song et al., 2020b) constructs prior distribution of the bivariate vector $\{\beta(s_j), \alpha(s_j)\}$ for each location s_j by thresholding a bivariate Gaussian latent vector $\{\tilde{\beta}(s_j), \tilde{\alpha}(s_j)\} \sim N_2(0, \Sigma)$ and their product. i.e.

$$\begin{aligned}\beta(s_j) &= \tilde{\beta}(s_j) \max \left\{ I(|\tilde{\beta}(s_j)| > \lambda_1), I(|\tilde{\beta}(s_j)\tilde{\alpha}(s_j)| > \lambda_0) \right\}, \\ \alpha(s_j) &= \tilde{\alpha}(s_j) \max \left\{ I(|\tilde{\alpha}(s_j)| > \lambda_2), I(|\tilde{\beta}(s_j)\tilde{\alpha}(s_j)| > \lambda_0) \right\}.\end{aligned}$$

PTG model uses the threshold parameters λ_1, λ_2 and λ_0 to control the sparsity in $\beta(s_j)$, $\alpha(s_j)$ and the indirect effect $\beta(s_j)\alpha(s_j)$ respectively, and Song et al. (2020b) directly set $\Sigma = \text{diag} \{\sigma_\beta^2, \sigma_\alpha^2\}$. However, the spatial correlation in spatially-varying coefficients among different locations s_j is not taken into consideration. Hence we anticipate this method to be less suitable for spatially correlated applications such as brain imaging. This method has been implemented in the R package `bama` (Rix et al., 2021). We set $\lambda_1 = \lambda_2 = \lambda_0 = 0.01$. A total number of 1500 MCMC iterations are performed with 1000 burnins.

Correlated Selection model (Song et al., 2020a, CorS) adopts a mixture model with four components to specify different sparsity patterns of $\alpha(s_j)$ and $\beta(s_j)$ and incorporate the

spatial correlations into prior specifications of mixing weights.

$$[\beta(s_j), \alpha(s_j)]^\top \sim \pi_1(s_j)\mathbf{N}_2(0, \mathbf{V}_1) + \pi_2(s_j)\mathbf{N}_2(0, \mathbf{V}_2) + \pi_3(s_j)\mathbf{N}_2(0, \mathbf{V}_3) + \pi_4(s_j)\boldsymbol{\delta}_0,$$

and a membership variable $\gamma(s_j) \in \{1, 2, 3, 4\}$, where $\gamma(s_j) = 1$ indicates $\beta(s_j)\alpha(s_j) \neq 0$, $\gamma(s_j) = 2$ indicates $\beta(s_j) \neq 0, \alpha(s_j) = 0$, $\gamma(s_j) = 3$ indicates $\beta(s_j) = 0, \alpha(s_j) \neq 0$, and $\gamma(s_j) = 4$ indicates $\beta(s_j) = \alpha(s_j) \neq 0$. When $\gamma(s_j) = 1$, \mathbf{V}_1 is assigned an inverse Wishart prior. When $\gamma(s_j) = 2$ or 3 , \mathbf{V}_2 or \mathbf{V}_3 only contains σ_β^2 or σ_α^2 on the diagonal and 0 otherwise. Each $\gamma(s_j)$ is assumed to follow a multinomial distribution with probability $\boldsymbol{\pi}(s_j) = \{\pi_1(s_j), \pi_2(s_j), \pi_3(s_j), \pi_4(s_j)\}^\top$ with $\sum_{k=1}^4 \pi_k(s_j) = 1$. For each $m = 1, 2, 3$, let $\boldsymbol{\pi}_m = \{\pi_m(s_1), \dots, \pi_m(s_j)\} \in \mathbb{R}^p$. $\text{logit}(\boldsymbol{\pi}_m)$ is assumed to follow a multivariate normal prior with a pre-specified covariance matrix $\sigma_m^2 \mathbf{D} \in \mathbb{R}^{p \times p}$, independently for each $m = 1, 2, 3$. Hence \mathbf{D} is used to reflect the mediator-wise correlation.

We anticipate this method to have good performance in the spatially correlated data application. We use the GitHub implementation of this method (https://github.com/yanyans7/Correlated_GMM_Mediation.git). In the simulation study, we set the initial values for all $\alpha(s)$ and $\beta(s)$ to be 0.5, the initial values for $\{\pi_k(s_j), k = 1, 2, 3, 4\}$ to be 0.25, the 2 by 2 scale matrix in Inverse-wishart prior for \mathbf{V}_1 to be $[1, 0.5; 0.5, 1]$, and the $p \times p$ matrix \mathbf{D} to be estimated from the input image correlations. A total number of 2000 MCMC iterations are performed with 1000 burn-ins.

Bayesian Image Mediation Analysis (BIMA) adopts a modified square-exponential kernel $\kappa(s, s'; a, b) = \text{cor}\{\beta(s), \beta(s')\} = \exp\{-a(s^2 + s'^2) - b\|s - s'\|^2\}$ with $a = 0.01$ and $b = 10$. We split the input image into four regions. We use Hermite polynomials up to the 10th degree, resulting in 66 basis coefficients to approximate each region. The initial values for all parameters are obtained from Gibbs sampling with Gaussian process priors for α and β . The threshold parameter $\nu = 0.5$ in STGP priors. For the outcome model (1), a total of 10^5 iterations are performed, with the acceptance probability tuned to be around 0.2 for

each region during the first 80% of burn-in iterations. The mediator model (2) follows the same setting, except with a total of 5000 iterations and a burn-in period comprising the first 90%.

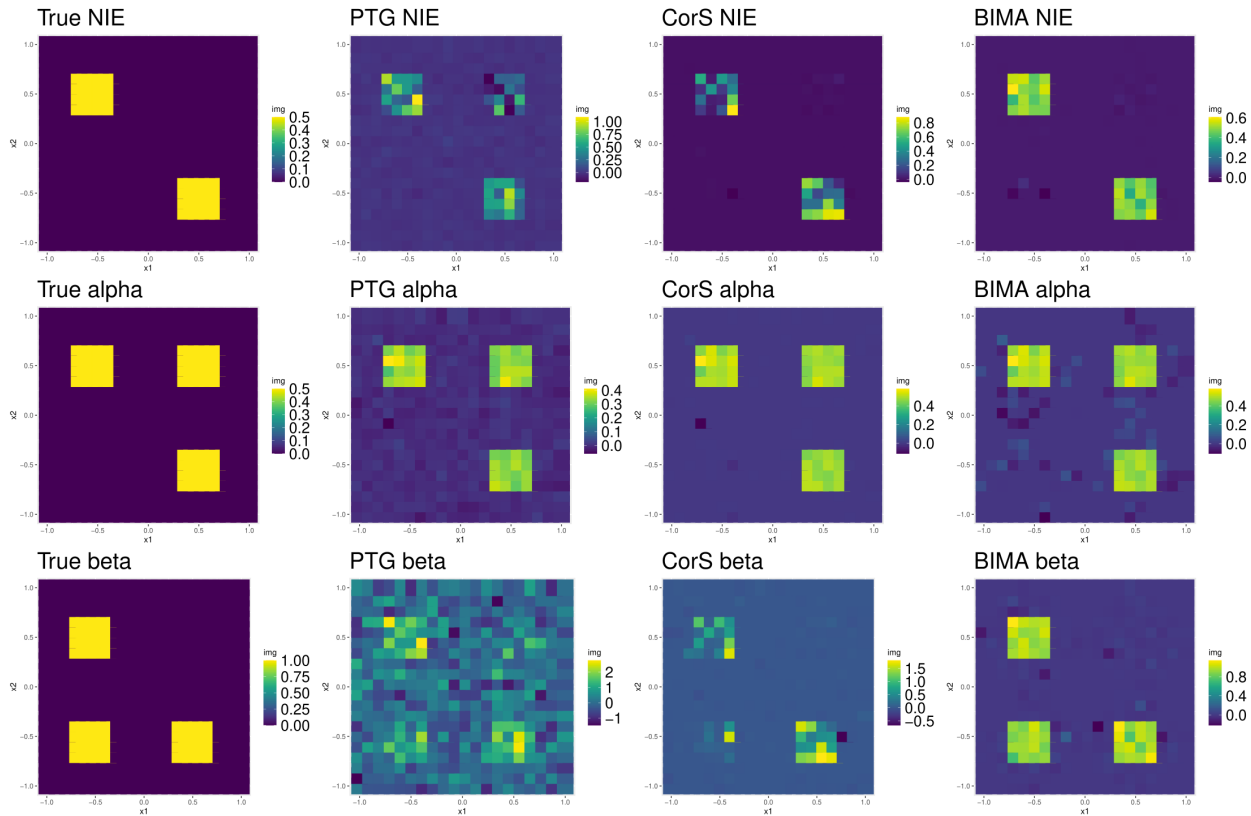


Figure 3: Comparison on the posterior mean of the 3 methods with the true images. Rows from top to bottom represent functional NIE $\mathcal{E}(s)$, $\alpha(s)$, $\beta(s)$. Columns from left to right represent true images, posterior mean from PTG model, posterior mean from CorS model, posterior mean from BIMA model.

Figure 3 shows the true image for $\alpha(s)$, $\beta(s)$, and $\mathcal{E}(s)$, i.e. natural indirect effect (NIE). Table 1 gives summary statistics of sampled NIE using 3 methods with 100 replicated simulations. The final result of NIE is tuned using the inclusion probability of the sampled NIE for all 3 methods in the following way: for each location s_j , we estimate the empirical probability $\hat{P}(\text{NIE}(s_j) \neq 0)$ from the MCMC sample of NIE, and set a threshold t on $\hat{P}(\text{NIE}(s_j) \neq 0)$: if $\hat{P}(\text{NIE}(s_j) \neq 0) < t$, $\text{NIE}(s_j) = 0$, otherwise $\text{NIE}(s_j)$ equals the posterior sample mean. By tuning t , we can control the FDR to be below 10%. Although we set the

target FDR to be 10% for all 3 methods, it is still possible that FDR cannot be tuned to be less than 10% with any $t < 1$ when the sample is very noisy, in which case the largest possible t is used, and the tuned FDR can be larger than 10%. In the extreme case where the largest possible t still maps all location to 0, we get the NAs as shown in Table 1. These NA replication results are excluded from the summary statistics in Table 1.

Table 1: Comparison of posterior inferences on NIE among different methods including PTG, CorS and BIMA based on 100 replications. The standard errors are reported in the brackets

(a) Selection accuracy including the overall accuracy (ACC), false discovery rate (FDR) and true positive rate (TPR). All values are multilied by 100.

Selection Accuracy									
(n, p)	PTG			CorS			BIMA		
	FDR	TPR	ACC	FDR	TPR	ACC	FDR	TPR	ACC
(200, 400)	9 (15)	20 (19)	93 (1)	1 (2)	80 (37)	98 (3)	7 (3)	95 (3)	99 (0)
(300, 400)	21 (21)	16 (14)	93 (1)	1 (2)	100 (0)	100 (0)	6 (3)	93 (5)	99 (0)
(200, 676)	14 (14)	11 (12)	93 (1)	0 (0)	3 (2)	93 (0)	8 (2)	96 (3)	99 (0)
(300, 676)	10 (14)	17 (11)	94 (1)	1 (1)	80 (36)	98 (3)	7 (2)	96 (3)	99 (0)

(b) Estimation and computation performance including mean squared errors (MSE) in the true activation region (multiplied by 100) and computation time in seconds.

Estimation and Computation time									
(n, p)	MSE (Activation)			Time (Seconds)				#of NA	
	PTG	CorS	BIMA	PTG	CorS	BIMA (1)	BIMA (2)	PTG	CorS
(200, 400)	24 (1)	5 (10)	2 (1)	251 (7)	26 (3)	27 (2)	28 (1)	31	7
(300, 400)	24 (1)	0 (0)	2 (1)	385 (8)	25 (2)	35 (3)	61 (1)	22	0
(200, 676)	24 (0)	25 (1)	2 (1)	663 (13)	75 (1)	54 (6)	35 (1)	60	60
(300, 676)	24 (0)	5 (9)	1 (1)	1026 (21)	76 (2)	64 (11)	71 (2)	21	11

From Table 1, PTG performs the least ideal in the correlated image setting as shown in Figure 3, especially in the estimation for the mediator effect $\beta(s)$. In general, $\beta(s)$ is more challenging to estimate than $\alpha(s)$ for two reasons: i) The mediator model (2) has $n \times p$ observations to estimate p dimensional $\alpha(s)$, leading to a higher signal to noise ratio than β in model (1); ii) In the outcome model (1), M and X are correlated through (2), making it more difficult to separate the effect $\beta(s)$ from γ .

CorS model performs very well when n is close to p . However in the higher dimensional setting, when n is much smaller than p , CorS has a lower power than BIMA. BIMA performs well and is stable across all four settings, indicating that it is a suitable method especially for high-dimensional spatially correlated mediators, when n is considerably less than p , such as in brain imaging application. Potential improvement can be made for BIMA when the kernel bases are tuned to accurately represent the smoothness of input mediators.

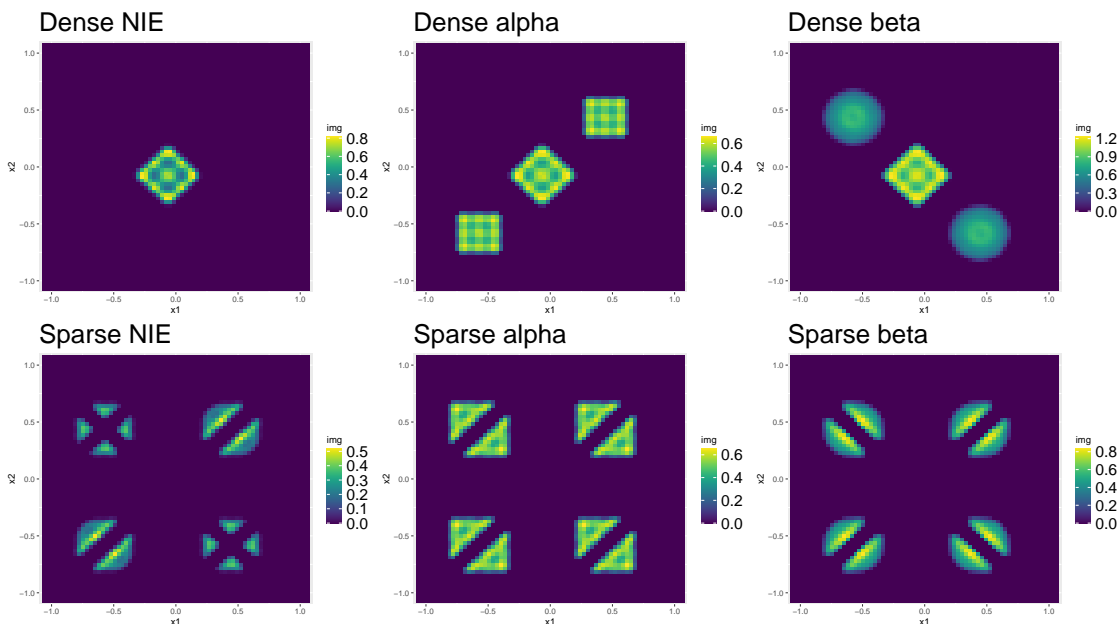


Figure 4: Input image pattern for the simulation study. Rows from top to bottom represent dense pattern and sparse pattern. Columns from left to right represent input image NIE, $\alpha(s)$, $\beta(s)$. $p = 4096$.

5.2 High-dimensional simulation

To further illustrate the performance of our proposed method, we conduct simulation studies under 4 different settings with 2 sets of patterns as shown in Figure 4. Each image is split into 4 regions, each region being a 32×32 grid. The threshold parameter $\nu = 0.5$ in STGP priors. In this simulation, we use Matérn kernel in accordance with the sharp patterns

in Figure 4.

$$\kappa(s', s; u, \rho) = C_u(\|s' - s\|_2^2/\rho), \quad C_u(d) := \frac{2^{1-u}}{\Gamma(u)} \left(\sqrt{2ud}\right)^u K_u(\sqrt{2ud}) \quad (9)$$

The number of basis for each region is set to be 20% of the region size. The scale parameter $\rho = 2$, and $u = 1/5$. Due to the high dimension of mediators, we let the MALA algorithm update only $\beta(s)$ for the first 40% of MCMC iterations to get $\beta(s)$ to a stable value, then jointly updating all other parameters in (1) using Gibbs Sampling. All other settings are the same as in Section 5.1, and the summary statistics for NIE in Table 2 are also tuned in the same way using inclusion probability. Table 2(b) gives a sensitivity analysis result using different thresholds ν in the STGP priors to show that the estimation is not too sensitive to the choice of ν within a small range.

Table 2 demonstrates that our proposed method has stable performance across different settings. In Table 2, the mediator model is fully updated and converged including all individual effects $(\eta_i)_{i=1}^n$. Fully updating $(\eta_i)_{i=1}^n$ can take much longer time for the entire model to converge compared to directly setting the individual effects all to 0. In the case all η_i fixed at 0, the estimation for α and ζ are almost the same compared to updating the full model from the $p = 4096$ simulation studies that we have observed. When $n = 1000$ and $p = 4096$, the computational time of fitting BIMA with running 30,000 MCMC iterations is less than four hours for both models (1) and (2). In comparison, the CorS method takes 9.8 hours when $N = 1000, p = 2000$, with 1.5×10^5 iterations. Our approach shows a much better computational efficiency in the high-dimensional setting.

6 Analysis of ABCD fMRI Data

In this section, we apply our method to the Adolescent Brain Cognitive Development (ABCD) study release 1 (Casey et al., 2018). The 2-back 3mm task fMRI contrast data is used, and the preprocessing method is described in Sripada et al. (2020). After preprocessing

Table 2: High-dimensional simulation results. Selection accuracy (multiplied by 100) includes false discovery rate (FDR), true positive rate (TPR) and overall accuracy (ACC). Computational time (in minutes) are separately reported for fitting model (1) (T1) and model (2) (T2). The reported values are the average over 100 replications. The standard deviations are reported in the brackets.

(a) Performance of BIMA in simulations for different sample sizes (n) and the random noise standard deviations in model (1) (σ_Y).

Under different generative model, $\lambda = 0.5$							
Pattern	n	σ_Y	FDR	TPR	ACC	T1	T2
Dense	1000	0.1	1 (1)	98 (1)	100 (0)	13 (2)	184 (16)
Sparse	1000	0.1	3 (3)	100 (0)	100 (0)	19 (4)	212 (28)
Dense	5000	0.1	1 (2)	97 (4)	100 (1)	54 (15)	1145 (140)
Dense	1000	0.5	1 (1)	98 (1)	100 (0)	17 (5)	209 (37)

(b) Sensitivity analysis with different threshold values (ν).

Under different sensitivity parameter ν .					
Dense pattern, $n = 1000$, $\sigma_Y = 0.1$.					
ν	FDR	TPR	ACC	T1	T2
0.3	5 (1)	99 (0)	99 (0)	20 (5)	198 (18)
0.6	0 (0)	97 (10)	100 (1)	17 (4)	222 (28)

and removing missing data, the final complete data set consists of $N = 1861$ subjects. The initial size of one image is $61 \times 73 \times 61$, which contains 116 brain regions, but only 90 regions are chosen for this application, and the resulting number of mediators in brain image is $p = 47636$.

We are interested in examining the natural indirect effect (NIE) of parental education level on children’s IQ scores, mediated through brain imaging data. Our aim is to explore the varying roles of different brain regions as mediators in the cognitive ability development of a child. Hence the exposure is a binary variable indicating whether the parent has a college or higher degree. The outcome variable is g-score that reflects children’s IQ, obtained in the same way as in [Sripada et al. \(2020\)](#) from the raw data. The confounders in our model include age, gender, race and ethnicity, and household income. For the multi-level variables

race and ethnicity (Asian, Black, Hispanic, Other, White), household income (less than 50k, between 50k and 100k, greater than 100k), we use binary coding for each level. Table 3 provides the summary statistics of the ABCD data.

Table 3: Summary statistics of the ABCD data stratified by Parent Degree. Mean (standard deviation) are reported for g-Score and Age. Counts are reported for Gender, Income, Race and Ethnicity

Parent degree	Bachelor or higher	No bachelor	Overall
g-Score	0.47 (0.77)	-0.15 (0.80)	0.27 (0.83)
Age	10.09 (0.61)	10.01 (0.63)	10.06 (0.62)
Gender			
Female	611	281	892
Male	635	334	969
Race and Ethnicity			
Asian	30	3	33
Black	47	84	131
Hispanic	151	216	367
White	924	254	1178
Other	94	58	152
Income			
<50K	98	336	434
50~100K	375	213	558
>=100K	773	66	839
Total	1246	615	1861

In this analysis, we use the Matérn kernel where the hyper-parameters u and ρ are specified for each region according to the estimated covariance matrices. The number of voxels for each region varies from 62 to 1510. To determine the number of basis, we select up to 500 locations within a certain range of the centroid for each region. Using these locations, we compute the empirical covariance matrix for each region. The cutoff for the number of basis is then chosen in such a way that it accounts for 90% of the total sum of all the singular values of the estimated covariance matrix. Because the hyper-parameter ν in the STGP prior and the kernel parameters u, ρ in each region are all prefixed, we provide a detailed description of selecting these parameters via testing MSE in the Supplementary

Material. The final threshold ν_β for $\beta(s)$ is set to be 0.05, and the final threshold ν_α for $\alpha(s)$ is set to be 0.1. The choice of ν is also based on testing MSE. Detailed sensitivity analysis can be found in the Supplementary Material.

A total of 100,000 iterations were performed for the outcome model (1) with the first 50% as burn-in, and thinning the posterior sample gives us 1000 samples out of the original 50,000 samples. A total of 40,000 iterations were performed for the mediator model (2) with the first 30,000 as burn-in, and the posterior sample are thinned every 10 iterations to have 1000 sample. Based on this 1000 posterior sample, Table 4 gives a summary of both the overall NIE and NDE and the top 7 regions identified with the largest number of active voxels. The definition of NIE in each region is $\frac{1}{p} \sum_{s \in \mathcal{S}_r} \beta(s)\alpha(s)$, where \mathcal{S}_r is the collection of all voxels in region r . The rule for selecting the active voxels is based on cutting the posterior inclusion probability (PIP) at 10%. Voxels with PIP values above this threshold are identified as active. The posterior of NDE γ has a mean of 0.27 with the 95% credible interval (0.20, 0.36). The posterior of NIE \mathcal{E} has a mean of 0.0885 with the 95% credible interval (0.066, 0.111). This suggests that parents with college degrees have a positive impact on children’s cognitive abilities, and about 25% of the effect is mediated through brain cognitive development. Figure 5 shows the estimated active regions and the NIE in coronal view slides.

7 Conclusion and Discussions

In this paper, we assign soft-thresholded Gaussian process priors on the spatial-varying coefficients in the outcome model and the mediator model. The thresholding parameter controls the sparsity of the functional coefficients, and the soft-thresholded operator provides a continuous mapping from the latent Gaussian process to the sparse coefficients. We extend the mediation analysis framework to incorporate spatial-varying mediators and provide theoretical guarantees on the posterior consistency of the functional natural indirect effect. Our computation approach utilizes the MALA algorithm, which is tailored to the imaging

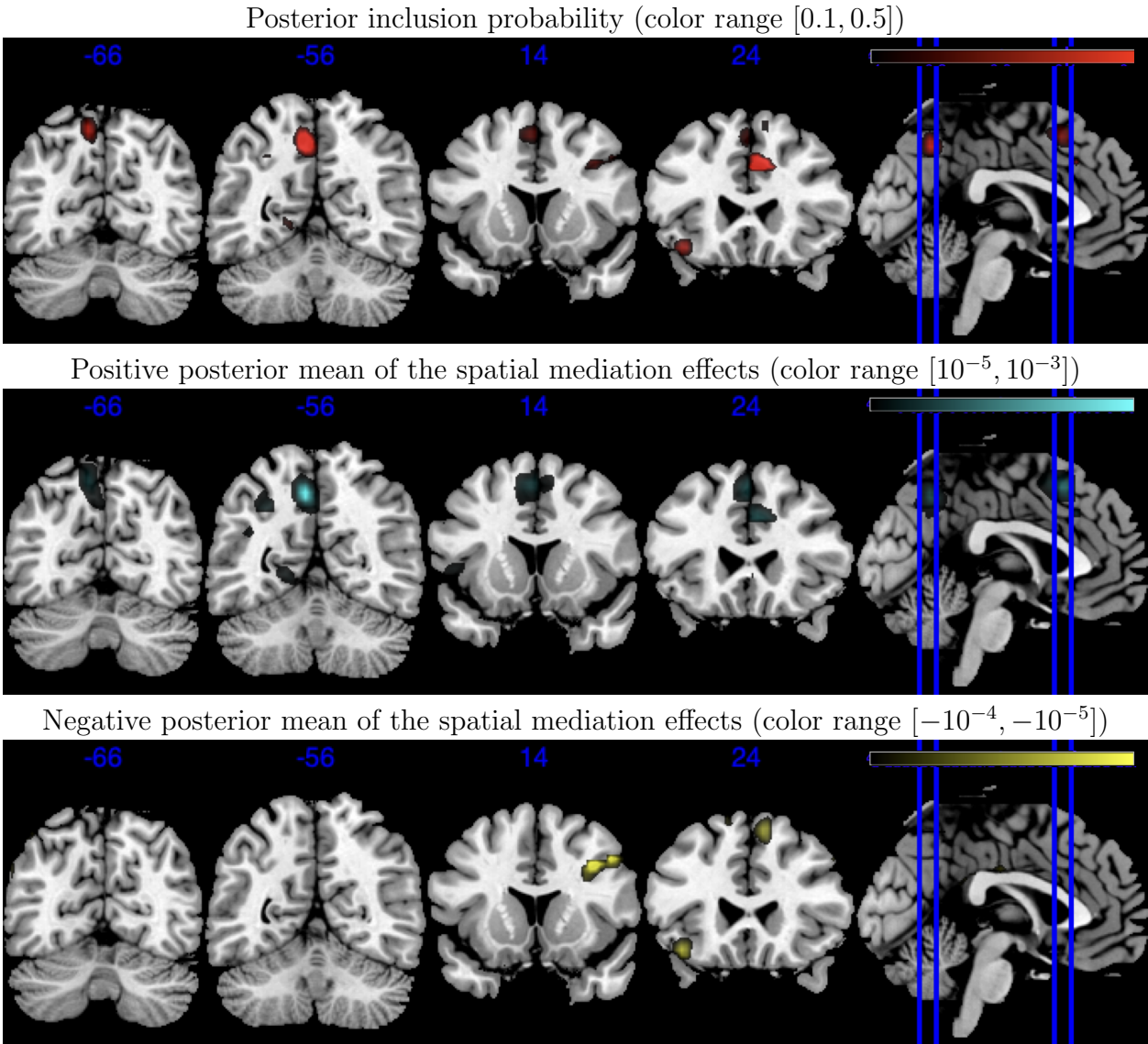


Figure 5: Posterior inference on spatially varying indirect effects of parental education on the general cognitive ability that are mediated through the working memory brain activity. The Coronal view slides cutting through 3 of the top 10 regions with largest number of active pixels: the left Precuneus (Precuneus.L), left Inferior parietal gyrus (Parietal_Inf.L) and the left Supplementary motor area (Supp_Motor_Area.L).

Table 4: Top 7 regions ordered by the number of active voxels with $PIP > 10\%$. Columns 2 to 5 are timed by 100. NIE(+) and NIE(-) are defined as $\frac{1}{p_n} \sum_{s \in \nabla_r} \mathcal{E}(s) I(\mathcal{E}(s) > 0)$ and $\frac{1}{p_n} \sum_{s \in \nabla_r} \mathcal{E}(s) I(\mathcal{E}(s) < 0)$ for each region r . Average IP is the averaged inclusion probability over all voxels in the entire region.

	NIE	NIE(+)	NIE(-)	NDE	Time (hours) model (1)	Time (hours) model (2)
Overall	8.85	10.57	-1.72	27.37	1.60	85.93
Region Name (AAL Atlas)	NIE	NIE(+)	NIE(-)	Average PIP	# of active voxels	Region Size
Precuneus_L	3.53	3.53	-0.01	4.98	109	1079
Parietal_Inf_L	2.83	2.83	0.00	5.67	99	696
Postcentral_L	0.21	0.21	0.00	1.98	71	1159
Cingulum_Mid_R	1.82	1.82	0.00	8.98	67	605
Supp_Motor_Area_L	1.14	1.16	-0.02	2.38	52	656
Frontal_Inf_Oper_R	-0.46	0.00	-0.47	1.83	27	421
Frontal_Inf_Orb_L	-0.12	0.02	-0.13	1.98	21	503

application with block updates.

Through small-scale simulation studies, we compare our method with existing approaches such as the Product Threshold Gaussian prior model (PTG) and the Correlated Selection model (CorS). We demonstrate that our method outperforms existing methods, particularly in scenarios involving high-dimensional correlated mediators. Furthermore, our implementation is more than four times faster than the CorS method when $N = 1000, p = 4096$. In the larger scale simulation where $p = 4096$, our proposed model performs better when the true signals are smoother and when there is lower variability in the outcome model but higher variability in the mediator model. We also apply our method to mediation analysis on ABCD data, demonstrating its applicability to other mediation problems involving imaging data or other types of high-dimensional mediation data, such as biomarker and genetic data.

However, there are several limitations to our proposed work. While the basis decomposition approach reduces the number of parameters to update, the choice of the appropriate number of basis still depends on the researcher’s discretion. The thresholding parameter ν is fixed and determined by the researcher a priori. Further improvements are needed in the sampling algorithm to handle higher-dimensional data, such as 2mm fMRI data with

mediators exceeding 2×10^5 .

References

- Armagan, A., Dunson, D. B., Lee, J., Bajwa, W. U., and Strawn, N. (2013), “Posterior consistency in linear models under shrinkage priors,” *Biometrika*, 100, 1011–1018.
- Casey, B., Cannonier, T., Conley, M. I., Cohen, A. O., Barch, D. M., Heitzeg, M. M., Soules, M. E., Teslovich, T., Dellarco, D. V., Garavan, H., et al. (2018), “The adolescent brain cognitive development (ABCD) study: imaging acquisition across 21 sites,” *Developmental cognitive neuroscience*, 32, 43–54.
- Chén, O. Y., Crainiceanu, C., Ogburn, E. L., Caffo, B. S., Wager, T. D., and Lindquist, M. A. (2018), “High-dimensional multivariate mediation with application to neuroimaging data,” *Biostatistics*, 19, 121–136.
- Choudhuri, N., Ghosal, S., and Roy, A. (2004), “Bayesian Estimation of the Spectral Density of a Time Series,” *Journal of the American Statistical Association*, 99, 1050–1059.
- Cong, Y., Chen, B., and Zhou, M. (2017), “Fast simulation of hyperplane-truncated multivariate normal distributions,” *Bayesian Analysis*, 12, 1017–1037.
- Durrett, R. (2019), *Probability: theory and examples*, vol. 49, Cambridge university press.
- Eddelbuettel, D. and François, R. (2011), “Rcpp: Seamless R and C++ Integration,” *Journal of Statistical Software*, 40, 1–18.
- Eddelbuettel, D. and Sanderson, C. (2014), “RcppArmadillo: Accelerating R with high-performance C++ linear algebra,” *Computational Statistics and Data Analysis*, 71, 1054–1063.
- Ghosal, S. and Roy, A. (2006), “Posterior consistency of Gaussian process prior for nonparametric binary regression,” *Ann. Statist.*, 34, 2413–2429.
- Ghosal, S. and van der Vaart, A. (2017), *Fundamentals of Nonparametric Bayesian Inference*, Cambridge Series in Statistical and Probabilistic Mathematics, Cambridge University Press.
- Guo, X., Li, R., Liu, J., and Zeng, M. (2022), “High-dimensional mediation analysis for selecting DNA methylation Loci mediating childhood trauma and cortisol stress reactivity,” *Journal of the American Statistical Association*, 1–32.

- Kang, J., Reich, B. J., and Staicu, A.-M. (2018), “Scalar-on-image regression via the soft-thresholded Gaussian process,” *Biometrika*, 105, 165–184.
- Lindquist, M. A. (2012), “Functional causal mediation analysis with an application to brain connectivity,” *Journal of the American Statistical Association*, 107, 1297–1309.
- Luo, C., Fa, B., Yan, Y., Wang, Y., Zhou, Y., Zhang, Y., and Yu, Z. (2020), “High-dimensional mediation analysis in survival models,” *PLoS computational biology*, 16, e1007768.
- MacKinnon, D. P. (2012), *Introduction to statistical mediation analysis*, Routledge.
- Nath, T., Caffo, B., Wager, T., and Lindquist, M. A. (2023), “A machine learning based approach towards high-dimensional mediation analysis,” *Neuroimage*, 268, 119843.
- Rix, A., Kleinsasser, M., and Song, Y. (2021), *bama: High Dimensional Bayesian Mediation Analysis*, r package version 1.2.
- Rubin, D. B. (1974), “Estimating causal effects of treatments in randomized and nonrandomized studies.” *Journal of educational Psychology*, 66, 688.
- (1980), “Randomization analysis of experimental data: The Fisher randomization test comment,” *Journal of the American Statistical Association*, 75, 591–593.
- Rudelson, M. and Vershynin, R. (2009), “Smallest singular value of a random rectangular matrix,” *Communications on Pure and Applied Mathematics: A Journal Issued by the Courant Institute of Mathematical Sciences*, 62, 1707–1739.
- Song, Y., Zhou, X., Kang, J., Aung, M. T., Zhang, M., Zhao, W., Needham, B. L., Kardia, S. L., Liu, Y., Meeker, J. D., et al. (2020a), “Bayesian Hierarchical Models for High-dimensional Mediation Analysis with Coordinated Selection of Correlated Mediators,” *arXiv preprint arXiv:2009.11409*.
- (2020b), “Bayesian Sparse Mediation Analysis with Targeted Penalization of Natural Indirect Effects,” *arXiv preprint arXiv:2008.06366*.
- Song, Y., Zhou, X., Zhang, M., Zhao, W., Liu, Y., Kardia, S. L., Roux, A. V. D., Needham, B. L., Smith, J. A., and Mukherjee, B. (2020c), “Bayesian shrinkage estimation of high dimensional causal mediation effects in omics studies,” *Biometrics*, 76, 700–710.

- Sripada, C., Angstadt, M., Rutherford, S., Taxali, A., and Shedden, K. (2020), “Toward a “treadmill test” for cognition: Improved prediction of general cognitive ability from the task activated brain,” *Human brain mapping*, 41, 3186–3197.
- van der Vaart, A. and van Zanten, H. (2011), “Information Rates of Nonparametric Gaussian Process Methods.” *Journal of Machine Learning Research*, 12, 2095–2119.
- VanderWeele, T. and Vansteelandt, S. (2014), “Mediation analysis with multiple mediators,” *Epidemiologic methods*, 2, 95–115.
- Vershynin, R. (2018), *High-dimensional probability: An introduction with applications in data science*, vol. 47, Cambridge university press.
- Williams, C. K. and Rasmussen, C. E. (2006), *Gaussian processes for machine learning*, MIT press Cambridge, MA.
- Yuan, Y. and MacKinnon, D. P. (2009), “Bayesian mediation analysis.” *Psychological methods*, 14, 301.
- Zhang, A. R. and Zhou, Y. (2020), “On the non-asymptotic and sharp lower tail bounds of random variables,” *Stat*, 9, e314.
- Zhang, H., Zheng, Y., Zhang, Z., Gao, T., Joyce, B., Yoon, G., Zhang, W., Schwartz, J., Just, A., Colicino, E., et al. (2016), “Estimating and testing high-dimensional mediation effects in epigenetic studies,” *Bioinformatics*, 32, 3150–3154.
- Zhao, Y., Lindquist, M. A., and Caffo, B. S. (2020), “Sparse principal component based high-dimensional mediation analysis,” *Computational statistics & data analysis*, 142, 106835.
- Zhao, Y. and Luo, X. (2019), “Granger mediation analysis of multiple time series with an application to functional magnetic resonance imaging,” *Biometrics*, 75, 788–798.
- (2022), “Pathway Lasso: pathway estimation and selection with high-dimensional mediators,” *Statistics and Its Interface*, 15, 39–50.

In this supplement, we provide the proof of Theorem 1 to 3, and the sensitivity analysis of the ABCD data under different kernel and thresholding parameters.

A Proof

A.1 Proof of Proposition 1

Proof of Proposition 1. In this proof we omit the notations $\mu_{M,i}$ to μ_i for simplicity. First we show the identifiability of model (2), namely part (a) in Proposition 1.

Consider two parameter sets $\Theta_M = \{\alpha, \{\zeta_k\}_{k=1}^q, \{\eta_i\}_{i=1}^n\}$ and $\Theta'_M = \{\alpha', \{\zeta'_k\}_{k=1}^q, \{\eta'_i\}_{i=1}^n\}$. Suppose the probability distributions of \mathbf{M} given \mathbf{X} and \mathbf{C} under Θ_M and Θ'_M are equal, i.e.,

$$\pi(\mathbf{M} \mid \mathbf{X}, \mathbf{C}, \Theta_M) = \pi(\mathbf{M} \mid \mathbf{X}, \mathbf{C}, \Theta'_M),$$

where \mathbf{X} and \mathbf{C} satisfy the Assumption 2. Note that $\mathbf{M} = \{M_i(s)\}$. The joint distributions of two multi-dimensional random variables are the same implies that the corresponding marginal distributions of any element of the two random variables are also the same. Hence we have for any $i \in \{1, \dots, n\}$ and any $s \in \mathcal{B}$,

$$\pi(M_i(s) \mid \mathbf{X}, \mathbf{C}, \Theta_M) = \pi(M_i(s) \mid \mathbf{X}, \mathbf{C}, \Theta'_M).$$

Since $M_i(s)$ follows a normal distribution, for $i \in \{1, \dots, n\}$ and any $s \in \mathcal{B}$,

$$\mu'_i(s) = \mu_i(s) \text{ and } \sigma_M'^2 = \sigma_M^2,$$

where $\mu_i(s) = \alpha(s)X_i + \eta_i(s) + \sum_{k=1}^q \zeta_k(s)C_{i,k}$ and $\mu'_i(s) = \alpha'(s)X_i + \eta'_i(s) + \sum_{k=1}^q \zeta'_k(s)C_{i,k}$. Consider the decomposition of $\mu_i(s)$, $\mu'_i(s)$, $\alpha(s)$, $\alpha'(s)$, $\eta_i(s)$ and $\eta'_i(s)$.

$$\begin{aligned} \mu_i(s) &= \sum_{l=1}^{\infty} \theta_{\mu,i,l} \psi_l(s), & \alpha(s) &= \sum_{l=1}^{\infty} \theta_{\alpha,l} \psi_l(s), & \eta_i(s) &= \sum_{l=1}^{\infty} \theta_{\eta,i,l} \psi_l(s), & \zeta_k(s) &= \sum_{l=1}^{\infty} \theta_{\zeta,k,l} \psi_l(s) \\ \mu'_i(s) &= \sum_{l=1}^{\infty} \theta_{\mu',i,l} \psi_l(s), & \alpha'(s) &= \sum_{l=1}^{\infty} \theta_{\alpha',l} \psi_l(s), & \eta'_i(s) &= \sum_{l=1}^{\infty} \theta_{\eta',i,l} \psi_l(s), & \zeta'_k(s) &= \sum_{l=1}^{\infty} \theta_{\zeta',k,l} \psi_l(s), \end{aligned}$$

where the basis coefficients are satisfied with the following identities.

$$\theta_{\mu,i,l} = \theta_{\alpha,l} X_i + \theta_{\eta,i,l} + \sum_{k=1}^q \theta_{\zeta,k,l} C_{i,k}, \quad \text{and} \quad \theta_{\mu',i,l} = \theta_{\alpha',l} X_i + \theta_{\eta',i,l} + \sum_{k=1}^q \theta_{\zeta',k,l} C_{i,k}.$$

Since $\mu_i(s) = \mu'_i(s)$ for any $i \in \{1, \dots, n\}$ and any $s \in \mathcal{B}$, then for any $l \geq 1$, $\theta_{\mu,i,l} = \theta_{\mu',i,l}$. Then we have $(\theta_{\alpha,l} - \theta_{\alpha',l})X_i + \theta_{\eta,1,l} - \theta_{\eta',1,l} + \sum_{k=1}^q (\theta_{\zeta,k,l} - \theta_{\zeta',k,l})C_{1,k} = 0$. According to the Assumption 2, for $t = 1, \dots, q+1$, $\sum_{i=1}^n W_{i,t}(\theta_{\eta,i,l} - \theta_{\eta',i,l}) = 0$. Let $\mathbf{b}_l = (\theta_{\alpha_1,l} - \theta'_{\alpha_1,l}, \theta_{\zeta_1,l} - \theta'_{\zeta_1,l}, \dots, \theta_{\zeta_q,l} - \theta'_{\zeta_q,l})$.

$\theta_{\zeta',1,l}, \dots, \theta_{\zeta,q,l} - \theta_{\zeta',q,l}, \theta_{\eta,1,l} - \theta'_{\eta,1,l}, \dots, \theta_{\eta,n,l} - \theta'_{\eta,n,l})^\top$ for any $l \geq 1$ and

$$\mathbf{A} = \begin{pmatrix} \mathbf{0}_{(q+1) \times 1} & \mathbf{0}_{(q+1) \times q} & \mathbf{W}^\top \\ \mathbf{X} & \mathbf{C} & \mathbf{I}_n \end{pmatrix},$$

where \mathbf{b}_l is of dimension $(q+1+n) \times 1$ and \mathbf{A} is of dimension $(n+q+1) \times (n+q+1)$. Then we have the linear system: $\mathbf{A}\mathbf{b}_l = \mathbf{0}_{(n+q+1) \times 1}$.

Denote $\tilde{\mathbf{X}} = (\mathbf{X}_{n \times 1}, \mathbf{C}_{n \times q}) \in \mathbb{R}^{n \times (q+1)}$. Note that $\det(\mathbf{A}) = \det(\mathbf{0} - \mathbf{W}^\top \mathbf{I}_n^{-1} \tilde{\mathbf{X}}) \det(\mathbf{I}_n) = \det(\mathbf{W}^\top \tilde{\mathbf{X}}) \neq 0$ by Assumption 2. This implies that $\mathbf{0}_{n+1+q}$ is the unique solution of $\mathbf{A}\mathbf{b}_l = \mathbf{0}_{n+1+q}$. Thus

$$\theta_{\alpha,l} = \theta_{\alpha',l}, \quad \theta_{\eta,i,l} = \theta_{\eta',i,l}, \quad \theta_{\zeta,k,l} = \theta_{\zeta',k,l}$$

This further implies that for any s and any i ,

$$\alpha(s) = \alpha'(s), \quad \eta_i(s) = \eta'_i(s), \quad \zeta_k(s) = \zeta'_k(s)$$

This proves the identifiability of model (2). Next, we show the statement in (b) in Proposition 1. Part (b) will be used in the proof of Theorem 1.

By directly setting $\mathbf{W} = \tilde{\mathbf{X}}$, and $\sum_{i=1}^n W_{i,t} \eta_i(s) = 0$ for $t = 1, \dots, q+1$, we know that $\sum_{i=1}^n \tilde{X}_{i,t} \eta_i(s) = 0$ for $t = 1, \dots, q+1$. For each s , let $\tilde{\boldsymbol{\alpha}}(s) = \{\alpha(s), \zeta_1(s), \dots, \zeta_q(s)\}^\top \in \mathbb{R}^{q+1}$ and $\tilde{\boldsymbol{\alpha}}'(s) = \{\alpha'(s), \zeta'_1(s), \dots, \zeta'_q(s)\}^\top \in \mathbb{R}^{q+1}$. Let $\tilde{\mathbf{b}}_l = (\theta_{\alpha_1,l} - \theta'_{\alpha_1,l}, \theta_{\zeta,1,l} - \theta_{\zeta',1,l}, \dots, \theta_{\zeta,q,l} - \theta_{\zeta',q,l})^\top$ and $\mathbf{g}_l = (\theta_{\eta,1,l} - \theta'_{\eta,1,l}, \dots, \theta_{\eta,n,l} - \theta'_{\eta,n,l})^\top$. Then $\tilde{\mathbf{X}}_i^\top \{\tilde{\boldsymbol{\alpha}}(s) - \tilde{\boldsymbol{\alpha}}'(s)\} = \sum_{l=1}^\infty \tilde{\mathbf{X}}_i^\top \tilde{\mathbf{b}}_l \psi_l(s)$ and $\tilde{\eta}_i(s) - \tilde{\eta}'_i(s) = \sum_{l=1}^\infty g_{l,i} \psi_l(s)$. Since $\int_S \{\mu_i(s) - \mu'_i(s)\}^2 \lambda(ds)$ is finite, by Fubini's theorem,

$$\begin{aligned} & \frac{1}{n} \sum_{i=1}^n \int_S \{\mu_i(s) - \mu'_i(s)\}^2 \lambda(ds) \\ &= \frac{1}{n} \int_S \sum_{i=1}^n \left\{ \tilde{\mathbf{X}}_i^\top (\tilde{\boldsymbol{\alpha}}(s) - \tilde{\boldsymbol{\alpha}}'(s)) \right\}^2 \lambda(ds) + \frac{1}{n} \int_S \sum_{i=1}^n \{\eta_i(s) - \eta'_i(s)\}^2 \lambda(ds) \\ &= \frac{1}{n} \int_S \sum_{i=1}^n \left\{ \left(\sum_{l=1}^\infty \tilde{\mathbf{X}}_i^\top \tilde{\mathbf{b}}_l \psi_l(s) \right)^2 + \left(\sum_{l=1}^\infty g_{l,i}^2 \psi_l(s) \right)^2 \right\} \lambda(ds) \\ &= \frac{1}{n} \sum_{i=1}^n \left\{ \sum_{l=1}^\infty (\tilde{\mathbf{X}}_i^\top \tilde{\mathbf{b}}_l)^2 + \sum_{l=1}^\infty g_{l,i}^2 \right\} \\ &= \frac{1}{n} \sum_{l=1}^\infty \|\tilde{\mathbf{X}} \tilde{\mathbf{b}}_l\|_2^2 + \frac{1}{n} \sum_{l=1}^\infty \|\mathbf{g}_l\|_2^2. \end{aligned}$$

By Assumption 2(a) that $\sigma_{\min}(\tilde{\mathbf{X}}) > \sqrt{n}$, $\|\tilde{\mathbf{X}}\tilde{\mathbf{b}}_l\|_2^2 \geq \sigma_{\min}^2(\tilde{\mathbf{X}})\|\tilde{\mathbf{b}}_l\|_2^2 \geq n\|\tilde{\mathbf{b}}_l\|_2^2$. Hence

$$\frac{1}{n} \sum_{i=1}^n \int_{\mathcal{S}} \{\mu_i(s) - \mu'_i(s)\}^2 \lambda(ds) \geq \sum_{l=1}^{\infty} \|\tilde{\mathbf{b}}_l\|_2^2 + \frac{1}{n} \sum_{l=1}^{\infty} \|\mathbf{g}_l\|_2^2.$$

Note that the empirical norm $\|f\|_{2,p}$ is a finite grid approximation of the Hilbert space inner product $\sqrt{\int_{\mathcal{S}} f^2(s) \lambda(ds)}$. By Definition 4(d), the approximation error is given by $err(f) = \left| \|f\|_{2,p}^2 - \int_{\mathcal{S}} f^2(s) \lambda(ds) \right| \leq Kp^{-2/d}$.

$$\begin{aligned} \|\alpha - \alpha'\|_{2,p}^2 &= \sum_{l=1}^{\infty} (\theta_{\alpha,l} - \theta_{\alpha',l})^2 + err(\alpha - \alpha') \\ \|\zeta_k - \zeta'_k\|_{2,p}^2 &= \sum_{l=1}^{\infty} (\theta_{\zeta_k,l} - \theta_{\zeta'_k,l})^2 + err(\zeta_k - \zeta'_k), \quad k = 1, \dots, q \\ \|\eta_i - \eta'_i\|_{2,p}^2 &= \sum_{l=1}^{\infty} (\theta_{\eta_i,l} - \theta_{\eta'_i,l})^2 + err(\eta_i - \eta'_i), \quad i = 1, \dots, n \end{aligned}$$

For n large enough such that $Kp^{-2/d} < \frac{1}{q+3}\epsilon^2$, the following inequality

$$\|\alpha(s) - \alpha'(s)\|_{2,p}^2 + \sum_{k=1}^q \|\zeta_k(s) - \zeta'_k(s)\|_{2,p}^2 + \frac{1}{n} \sum_{i=1}^n \|\eta_i(s) - \eta'_i(s)\|_{2,p}^2 > \epsilon^2$$

implies that there exists constant $c'_1 \sum_{l=1}^{\infty} \|\tilde{\mathbf{b}}_l\|_2^2 + n^{-1} \sum_{l=1}^{\infty} \|\mathbf{g}_l\|_2^2 > c'_1 \epsilon^2$ which further implies that there exists constant c_0 ,

$$\frac{1}{n} \sum_{i=1}^n \|\mu_i(s) - \mu'_i(s)\|_{2,p}^2 > c_0 \epsilon^2$$

Hence Proposition 1(b) follows. □

A.2 Proof of Theorem 1

Theorem 1 is proved by checking the conditions in Theorem A.1 in Choudhuri et al. (2004).

For simplicity, throughout the proof of Theorem 1, we use the following notations: $\theta = \{\alpha, \{\zeta_k\}_{k=1}^q, \{\eta_i\}_{i=1}^n\}$, and the true parameters denoted as $\theta_0 = \{\alpha_0, \{\zeta_k^0\}_{k=1}^q, \{\eta_i^0\}_{i=1}^n\}$. In addition, let $\mu_i(s) = \alpha(s)X_i + \sum_{k=1}^q \zeta_k(s)C_{i,k} + \eta_i(s)$ be the mean function given $\{X_i, \{C_{i,k}\}_{k=1}^q\}_{i=1}^n$, and $\mu_i^0(s)$ be the mean function under the true parameters.

Conditional on $\{X_i, \{C_{i,k}\}_{k=1}^q\}_{i=1}^n$, for individual i and location s_j , $M_i(s_j)$ follows independent distributions across $i = 1, \dots, n, j = 1, \dots, p$, with density function $\pi(M_i(s_j); \theta) = \phi(\mu_i(s_j), \sigma^2)$, where $\phi(\mu_i(s_j), \sigma^2)$ is used to denote the normal density with mean $\mu_i(s_j)$ and variance σ^2 . Let $\Lambda_{i,j}(\theta_0, \theta) := \log\{\pi(M_i(s_j); \theta_0)/\pi(M_i(s_j); \theta)\}$.

First, we verify the prior positivity condition as follows.

Lemma 1. (*Prior positivity condition*) *There exists a set B , $\Pi(B) > 0$ such that*

1. $\liminf_{\{n,p\} \rightarrow \infty} \Pi \left\{ \theta \in B : (np)^{-1} \sum_{i=1}^n \sum_{j=1}^p \mathbb{E}_{\theta_0} \{ \Lambda_{i,j}(\theta_0, \theta) \} < \epsilon \right\} > 0$ for all $\epsilon > 0$; and
2. $(np)^{-2} \sum_{i=1}^n \sum_{j=1}^p \text{Var}_{\theta_0} \{ \Lambda_{i,j}(\theta_0, \theta) \} \rightarrow 0$, as $n \rightarrow \infty$ and $p \rightarrow \infty$, for all $\theta \in B$.

Proof. Define

$$\|\theta - \theta_0\|_\infty = \max \left\{ \sup_{s \in \mathcal{S}} |\alpha(s) - \alpha_0(s)|, \max_k \sup_{s \in \mathcal{S}} |\zeta_k(s) - \zeta_k^0(s)|, \max_i \sup_{s \in \mathcal{S}} |\eta_i(s) - \eta_i^0(s)| \right\}. \quad (10)$$

For constant $\delta > 0$, consider

$$B_\delta = \{ \theta \in \Theta : \|\theta - \theta_0\|_\infty < \delta \}.$$

Since the prior distributions for the above parameters are independent, to show $\Pi(B_\delta) > 0$, we only need to show that the prior of each term in (10) being upper bounded by a constant has a positive probability.

By Theorem 4 in Ghosal and Roy (2006), for any $i = 1, \dots, n, k = 1, \dots, q$,

$$\Pi \left(\sup_{s \in \mathcal{S}} |\eta_i(s) - \eta_i^0(s)| < \delta \right) > 0, \quad \Pi \left(\sup_{s \in \mathcal{S}} |\zeta_k(s) - \zeta_k^0(s)| < \delta \right) > 0.$$

By Lemma 2 in Kang et al. (2018), for any threshold $\nu > 0$ and any true $\alpha_0(s) \in \Theta_\alpha$, there exists $\tilde{\alpha}(s)$ in the RKHS of $\kappa(\cdot, \cdot)$ such that $\alpha_0 = T_\nu(\tilde{\alpha}_0)$. Note that the soft-thresholding function $T_\nu(x)$ is a 1-Lipschitz continuous function of x , and by Theorem 4 in Ghosal and Roy (2006), we have $\Pi(\sup_{s \in \mathcal{S}} |\tilde{\alpha}(s) - \tilde{\alpha}_0(s)| < \delta) > 0$, which implies $\Pi(\sup_{s \in \mathcal{S}} |T_\nu(\tilde{\alpha}(s)) - T_\nu(\tilde{\alpha}_0(s))| < \delta) > 0$. Hence for any $\theta \in B_\delta$, where $\Pi(B_\delta) > 0$, we

have

$$\begin{aligned}
\mathbb{E}_{\theta_0} [\Lambda_{i,j}(\theta_0, \theta)] &= \mathbb{E} [\mathbb{E}_{\theta_0} \{ \Lambda_{i,j}(\theta_0, \theta) \mid \mathbf{X}, \mathbf{C} \}] \\
&= -\frac{1}{2\sigma_M^2} \mathbb{E} [\mathbb{E}_{\theta_0} \{ (M_i(s_j) - \mu_i^0(s_j))^2 \mid \mathbf{X}, \mathbf{C} \}] \\
&\quad + \frac{1}{2\sigma_M^2} \mathbb{E} [\mathbb{E}_{\theta_0} \{ (M_i(s_j) - \mu_i^0(s_j) + \mu_i^0(s_j) - \mu_i(s_j))^2 \mid \mathbf{X}, \mathbf{C} \}] \\
&= \mathbb{E} \left[\frac{1}{2\sigma_M^2} (\mu_i^0(s_j) - \mu_i(s_j))^2 \right]
\end{aligned}$$

Note that

$$\begin{aligned}
&\frac{1}{2\sigma_M^2} \{ \mu_i^0(s_j) - \mu_i(s_j) \}^2 \\
&\leq \frac{1}{2\sigma_M^2} \left[\{ \alpha(s_j) - \alpha_0(s_j) \} X_i + \sum_{k=1}^q \{ \zeta_k(s_j) - \zeta_k^0(s_j) \} C_{i,k} + \{ \eta_i(s_j) - \eta_i^0(s_j) \} \right]^2 \\
&\leq \frac{2}{\sigma_M^2} \left[X_i^2 \{ \alpha(s_j) - \alpha_0(s_j) \}^2 + \sum_{k=1}^q \{ \zeta_k(s_j) - \zeta_k^0(s_j) \}^2 C_{i,k}^2 + \{ \eta_i(s_j) - \eta_i^0(s_j) \}^2 \right]
\end{aligned}$$

By choosing a constant K_{\max} such that $\max_i \{ \mathbb{E} \{ |X_i|^2 \} \}, \max_k \mathbb{E} \{ |C_{i,k}|^2 \} \leq K_{\max}$, then for any $\theta \in B_\delta$, $(np)^{-1} \sum_{i=1}^n \sum_{j=1}^p \mathbb{E}_{\theta_0} \{ \Lambda_{i,j}(\theta_0, \theta) \} < 2\sigma_M^{-2} K_{\max} (2+q) \delta^2$, hence for a small enough ϵ such that $0 < \epsilon < \sigma_M^{-2} K_{\max} (2+q) \delta^2$,

$$\begin{aligned}
&\liminf_{\{n,p\} \rightarrow \infty} \Pi \left\{ \theta \in B_\delta : \frac{1}{np} \sum_{i=1}^n \sum_{j=1}^p \mathbb{E}_{\theta_0} (\Lambda_{i,j}(\theta_0, \theta)) < \epsilon \right\} \\
&\geq \Pi \left\{ \|\theta - \theta_0\|_\infty \leq \sqrt{\left(\frac{2}{\sigma_M^2} K_{\max} (2+q) \right)^{-1} \epsilon} \right\} > 0.
\end{aligned}$$

To show the second condition, we only need to show that for any i, j and any $\theta \in B_\delta$, the variance $\text{Var}_{\theta_0} \{ \Lambda_{i,j}(\theta_0, \theta) \}$ is bounded by some constant.

$$\begin{aligned}
\text{Var}_{\theta_0} \{ \Lambda_{i,j}(\theta_0, \theta) \} &= \mathbb{E} \{ \text{Var}_{\theta_0} \{ \Lambda_{i,j}(\theta_0, \theta) \mid \mathbf{X}, \mathbf{C} \} \} + \text{Var} \{ \mathbb{E}_{\theta_0} \{ \Lambda_{i,j}(\theta_0, \theta) \mid \mathbf{X}, \mathbf{C} \} \} \\
&= \mathbb{E} \left\{ \frac{1}{\sigma_M^2} (\mu_i^0(s_j) - \mu_i(s_j))^2 \right\} + \text{Var} \left\{ \frac{1}{2\sigma_M^2} (\mu_i^0(s_j) - \mu_i(s_j))^2 \right\} \\
&\leq \max \left\{ \frac{4}{\sigma_M^2} K_{\max} (2+q) \delta^2, \frac{4}{\sigma_M^4} K_{\max, V} (2+q) \delta^4 \right\} < \infty,
\end{aligned}$$

where $K_{\max, V} \geq \max_i \{ \text{Var}(X_i^2), \max_k \text{Var}(C_{i,k}^2) \}$.

□

Before the test construction, we add a useful lemma on the tail probability of the maximum of sub-Gaussian random variables.

Lemma 2. *Let $X_i, i = 1, \dots, N$ be sub-Gaussian random variables. Let σ_i^2 be the constant such that $\mathbb{P}(|X_i| > t) \leq 2 \exp(-t^2/\sigma_i^2)$ for any $t > 0$ and $i = 1, \dots, N$. Let $\tilde{\sigma}_N^2 = \bigvee_{i=1}^N \sigma_i^2$. Then for any $t > 0$, $\mathbb{P}\left(\max_i |X_i| > \sqrt{\tilde{\sigma}_N^2 \log 2N + t}\right) \leq \exp(-t)$.*

Proof. Let $u = \sqrt{\tilde{\sigma}_N^2 \log 2N + t}$,

$$\mathbb{P}\left(\max_i |X_i| > u\right) \leq \sum_i \mathbb{P}(|X_i| > u) \leq 2N \exp\{-u^2/\tilde{\sigma}_N^2\} = \exp(-t).$$

□

Next, we construct a test that satisfies the Type I and Type II error bound on a specified sieve space.

Lemma 3. *(Existence of tests) There exist test functions $\{\Phi_{np}\}$, subset $\mathcal{U}_n, \Theta_n \subset \Theta$, and constant $K_1, K_2, c_1, c_2 > 0$ such that*

$$(a) \mathbb{E}_{\theta_0} \Phi_{np} \rightarrow 0, \text{ as } n \rightarrow \infty \text{ and } p \rightarrow \infty;$$

$$(b) \sup_{\theta \in \mathcal{U}_n^c \cap \Theta_n} \mathbb{E}_{\theta}(1 - \Phi_{np}) \leq K_1 e^{-c_1 np};$$

$$(c) \Pi(\Theta_n^c) \leq K_2 e^{-c_2 np}.$$

Proof. Define the sieve space of θ as Θ_n , which be decomposed into product of the following parameter space:

$$\begin{aligned} \Theta_n &= \Theta_{\alpha, n} \times \prod_{k=1}^q \Theta_{\zeta, k, n} \times \prod_{i=1}^n \Theta_{\eta, i, n} \\ \Theta_{\alpha, n} &= \left\{ \alpha \in \Theta_{\alpha} : \sup_{s \in \mathcal{R}_1 \cup \mathcal{R}_{-1}} \|D^{\omega} \alpha(s)\|_{\infty} < \sqrt{np}, \|\omega\|_1 \leq \rho \right\} \\ \Theta_{\zeta, k, n} &= \left\{ \zeta_k \in \Theta_{\zeta} : \sup_{s \in \mathcal{S}} \|D^{\omega} \zeta_k(s)\|_{\infty} < np, \|\omega\|_1 \leq \rho \right\}, k = 1, \dots, q \\ \Theta_{\eta, i, n} &= \left\{ \eta_i \in \Theta_{\eta} : \sup_{s \in \mathcal{S}} \|D^{\omega} \eta_i(s)\|_{\infty} < np, \|\omega\|_1 \leq \rho \right\}, i = 1, \dots, n \end{aligned}$$

where $D^{\omega} f(s)$ stands for $(\partial^{\|\omega\|_1} / \partial \omega^1, \dots, \partial^{\|\omega\|_1} / \partial \omega^d) f(s)$ for any $\omega = (\omega_1, \dots, \omega_d)^T$ with $\omega_j (j = 1, \dots, d)$ being positive intergers and $s \in \mathbb{R}^d$.

To show the conditions (a) and (b), we use Lemma 8.27(i) in [Ghosal and van der Vaart \(2017\)](#), by viewing $\mathbf{M} \sim N_{np}(\boldsymbol{\mu}, \sigma^2 I)$, $\boldsymbol{\mu} = \{\mu_i(s_j)\}_{i=1, j=1}^{n, p} \in \mathbb{R}^{np}$. By Lemma 8.27(i), for any $\boldsymbol{\mu}_1, \boldsymbol{\mu}_0 \in \mathbb{R}^{np}$, there exists $\Phi(\boldsymbol{\mu}_1)$ such that for any $\boldsymbol{\mu}$ where $\|\boldsymbol{\mu} - \boldsymbol{\mu}_1\|_2 \leq \|\boldsymbol{\mu}_0 - \boldsymbol{\mu}_1\|_2/2$,

$$\mathbb{E}_{\boldsymbol{\mu}_0} \Phi(\boldsymbol{\mu}_1) \vee \mathbb{E}_{\boldsymbol{\mu}} \{1 - \Phi(\boldsymbol{\mu}_1)\} \leq \exp \left\{ -c_1 \|\boldsymbol{\mu}_0 - \boldsymbol{\mu}_1\|_2^2 / \sigma_M^2 \right\}$$

Because the type II error in condition (b) does not depend on a single $\boldsymbol{\mu}_1$, to remove the dependence on $\boldsymbol{\mu}_1$, and to use a neighborhood \mathcal{U}_n defined by the empirical norm as the distance metric instead of the Euclidean norm, we use the same technique as the one in Proposition 11 in [van der Vaart and van Zanten \(2011\)](#). For any $r \geq 1$, any integer $j \geq 1$, define shells for $\boldsymbol{\mu}$

$$\mathcal{C}_{j,r} := \{\Theta_n : jr \leq \|\boldsymbol{\mu} - \boldsymbol{\mu}_0\|_2 \leq (j+1)r\}$$

Denote $\mathcal{P}(\mathcal{C}_{j,r}, jr/2, \|\cdot\|_2)$ as the largest packing number of $\mathcal{C}_{j,r}$ with Euclidean distance $jr/2$, and denote the corresponding $jr/2$ -separated set of $\mathcal{C}_{j,r}$ as \mathcal{P}_j . Note that \mathcal{P}_j is also a $jr/2$ -covering set of $\mathcal{C}_{j,r}$. Hence for any $\boldsymbol{\mu} \in \mathcal{C}_{j,r}$, there exists $\boldsymbol{\mu}_1 \in \mathcal{P}_j$ such that

$$\|\boldsymbol{\mu} - \boldsymbol{\mu}_1\|_2 \leq \frac{jr}{2} \leq \frac{1}{2} \|\boldsymbol{\mu}_1 - \boldsymbol{\mu}_0\|_2.$$

Choose $\Phi_j = \max_{\boldsymbol{\mu}_1 \in \mathcal{P}_j} \{\Phi(\boldsymbol{\mu}_1)\}$, then for any $\boldsymbol{\mu} \in \mathcal{C}_{j,r}$, conditioning on \mathbf{X}, \mathbf{C} ,

$$\begin{aligned} \mathbb{E}_{\boldsymbol{\mu}_0, \sigma_0} \Phi_j &\leq 2\mathcal{P}(\mathcal{C}_{j,r}, \frac{jr}{2}, \|\cdot\|_2) \exp \left\{ -c_1 [(jr)^2] / \sigma_M^2 \right\} \\ \mathbb{E}_{\boldsymbol{\mu}, \sigma} (1 - \Phi_j) &\leq \exp \left\{ -c_1 [(jr)^2] / \sigma_M^2 \right\} \end{aligned}$$

Denote $\mathcal{N}(\Theta_n, r, \|\cdot\|_\infty)$ as the smallest covering number for the set Θ_n with radius r and distance function $\|\cdot\|_\infty$. Now we need an upper bound on $\log \mathcal{N}(\Theta_n, r, \|\cdot\|_\infty)$. Note that by Lemma 2 in [Ghosal and Roy \(2006\)](#) and a similar approach in Lemma A1 in [Kang et al. \(2018\)](#), there exist constants $K_\alpha, K_\zeta, K_\eta$, such that $\log \mathcal{N}(\Theta_{\alpha, n}, r, \|\cdot\|_\infty) \leq K_\alpha (np)^{d/(2\rho)} r^{-d/\rho}$, and $\log \mathcal{N}(\Theta_{\eta, i, n}, r, \|\cdot\|_\infty) \leq K_\eta (np)^{d/\rho} r^{-d/\rho}$, $\log \mathcal{N}(\Theta_{\zeta, k, n}, r, \|\cdot\|_\infty) \leq K_\zeta (np)^{d/\rho} r^{-d/\rho}$. Hence

there exists constant K_0 ,

$$\begin{aligned}
& \log \mathcal{N}(\Theta_n, r, \|\cdot\|_\infty) \\
& \leq \log \mathcal{N}(\Theta_{\alpha,n}, r, \|\cdot\|_\infty) + \sum_{k=1}^q \log \mathcal{N}(\Theta_{\zeta,k,n}, r, \|\cdot\|_\infty) + \sum_{i=1}^n \log \mathcal{N}(\Theta_{\eta,i,n}, r, \|\cdot\|_\infty) \\
& \leq K_0 n(np)^{d/\rho} r^{-d/\rho}
\end{aligned}$$

Conditioning on (\mathbf{X}, \mathbf{C}) , denote

$$\Theta_n^* := \left\{ \boldsymbol{\mu} \in \mathbb{R}^{np} : \mu_{ij} = \alpha(s_j)X_i + \sum_{k=1}^q \zeta_k(s_j)C_{i,k} + \eta_i(s_j), \theta \in \Theta_n \right\}.$$

Now we first show that conditioning on (\mathbf{X}, \mathbf{C}) , given $c_n^* = \max_i \{|X_i|, \|\mathbf{C}_i\|_\infty\}$,

$$\log \mathcal{N}(\Theta_n^*, r/(4\sqrt{np}), \|\cdot\|_\infty) \leq \log \mathcal{N}(\Theta_n, r/(4c_n^*\sqrt{np}), \|\cdot\|_\infty).$$

Denote $\mathcal{S}_{\mu,n}^*$ as a (c_n^*r) -covering set of Θ_n^* under $\|\cdot\|_\infty$. $\mathcal{S}_{\mu,n}^*$ is constructed in the following way: for any $\boldsymbol{\mu} \in \Theta_n^*$, there exists a corresponding $\theta_\mu = (\alpha, \{\zeta_k\}_{k=1}^q, \{\eta_i\}_{i=1}^n) \in \Theta_n$ such that $\mu_{ij} = \alpha(s_j)X_i + \sum_{k=1}^q \zeta_k(s_j)C_{i,k} + \eta_i(s_j)$, hence there exists $\theta_{\mu,1} \in \mathcal{N}_{\mu,n}$ where $\mathcal{N}_{\mu,n}$ is the smallest covering set with cardinality $\mathcal{N}(\Theta_n, r, \|\cdot\|_\infty)$, and there exists corresponding $\boldsymbol{\mu}_1 \in \Theta_n^*$ given θ_1 .

$$|\mu_{1,ij} - \mu_{ij}| \leq |(\alpha(s_j) - \alpha_1(s_j))X_i| + \sum_{k=1}^q |(\zeta_k(s_j) - \zeta_{1,k}(s_j))C_{i,k}| + |\eta_i(s_j) - \eta_{1,i}(s_j)| \leq c_n^*r$$

Hence $\mathcal{S}_{\mu,n}^*$ can be constructed as a collection of all such $\boldsymbol{\mu}_1$. Let $|\mathcal{S}_{\mu,n}^*|$ be the cardinality of such $\mathcal{S}_{\mu,n}^*$. By the construction of $\mathcal{S}_{\mu,n}^*$, $|\mathcal{S}_{\mu,n}^*| \leq \mathcal{N}(\Theta_n, r, \|\cdot\|_\infty)$.

Since $\|\cdot\|_{2,np} \leq \|\cdot\|_\infty$, we have

$$\begin{aligned}
\log \mathcal{P}(\Theta_n^*, r/2, \|\cdot\|_2) & \leq \log \mathcal{N}(\Theta_n^*, r/4, \|\cdot\|_2) = \log \mathcal{N}(\Theta_n^*, r/(4\sqrt{np}), \|\cdot\|_{2,np}) \\
& \leq \log \mathcal{N}(\Theta_n^*, r/(4\sqrt{np}), \|\cdot\|_\infty) \leq \log |\mathcal{S}_{\mu,n}^*| \\
& \leq \log \mathcal{N}(\Theta_n, r/(4c_n^*\sqrt{np}), \|\cdot\|_\infty) \\
& \leq K_0 (4c_n^*)^{d/\rho} n(np)^{3d/(2\rho)} r^{-d/\rho}
\end{aligned} \tag{11}$$

Denote event $A = \left[c_n^* < a\sqrt{\log \{n\}} \right]$ and I_A be its indicator, where a is an absolute constant, Lemma 2 implies that $\mathbb{P}(I_{A^c}) \rightarrow 0$ as $n \rightarrow \infty$, where A^c denotes the complement of A . Hence

given A , $\log \mathcal{P}(\Theta_n^*, r/2, \|\cdot\|_2) \leq K_a (\log n)^{d/(2\rho)} n(np)^{3d/(2\rho)} r^{-d/\rho}$.

Then for any $\boldsymbol{\mu} \in \cup_{j \geq 1} \mathcal{C}_{j,r}$, $\sigma \in \cup_{j \geq 1} \mathcal{C}_{j,\epsilon}$, define $\Phi = \sum_{j \geq 1} \Phi_j I(\boldsymbol{\mu} \in \mathcal{C}_{j,r})$, for some constants K_2, K_3 , conditioning on \mathbf{X}, \mathbf{C} ,

$$\begin{aligned}
\mathbb{E}_{\boldsymbol{\mu}_0} \Phi &\leq \sum_{j \geq 1} 2\mathcal{P}(\mathcal{C}_{j,r}, jr/2, \|\cdot\|_2) \exp\{-c_1[(jr)^2]/\sigma_M^2\} \\
&\leq 2\mathcal{P}(\Theta_n^*, r/2, \|\cdot\|_2) \sum_{j \geq 1} \exp\{-c_1[j(r)^2]/\sigma_M^2\} \\
&\leq 2\mathcal{P}(\Theta_n^*, r/2, \|\cdot\|_2) K_2 \exp\left(-\frac{c_1 r^2}{4\sigma_M^2}\right) \\
&\leq K_3 \mathcal{P}(\Theta_n^*, r/2, \|\cdot\|_2) \exp\left(-\frac{c_1 r^2}{\sigma_M^2}\right) \\
\mathbb{E}_{\boldsymbol{\mu}}(1 - \Phi) &\leq \sum_{j \geq 1} \exp\{-c_1[(jr)^2]\} (2\sigma_M^2)^{-1} \\
&\leq K_3 \exp\left\{-\frac{c_1 r^2}{\sigma_M^2}\right\}
\end{aligned}$$

Choose $r = \sqrt{np}\epsilon$, for any $\epsilon > 0$, we can choose n, p large enough such that $r > 1$. By Proposition 1(b), $\mathcal{U}_M^c \subset \mathcal{U}_{M,1}^c$ almost surely, where

$$\begin{aligned}
\mathcal{U}_M^c &= \left\{ \Theta : \|\alpha(s) - \alpha_0(s)\|_{2,p}^2 + \sum_{k=1}^q \|\zeta_k(s) - \zeta_{k,0}(s)\|_p^2 + \frac{1}{n} \sum_{i=1}^n \|\eta_i(s) - \eta_i(s)\|_{2,p}^2 > \epsilon^2 \right\} \\
\mathcal{U}_{M,1}^c &= \{\Theta : \|\boldsymbol{\mu} - \boldsymbol{\mu}_0\|_{2,np} > \sqrt{c_0}\epsilon\}
\end{aligned}$$

Then for any $\theta \in \Theta_n \cap \mathcal{U}_{M,1}^c$, note that $(\log n)^{d/(2\rho)}(np)^{d/\rho} < n^{d/(2\rho)}(np)^{d/\rho} < p$ given Assumption 1, $\rho > d + 3/(2\tau)$.

$$\begin{aligned}
\mathbb{E}\{\mathbb{E}_{\boldsymbol{\mu}_0, \sigma_0}\{\Phi \mid \mathbf{X}, \mathbf{C}\}\} &\leq \mathbb{E}_A\{\mathcal{P}(\Theta_n^*, \sqrt{np}c_0\epsilon/2, \|\cdot\|_2)\} K_4 \exp\{-c_1'' np\epsilon^2\} + \mathbb{E}\{I_{A^c}\} \\
&\leq K' \exp\left\{c_1''' (\log n)^{d/(2\rho)} n(np)^{d/\rho} \epsilon^{-d/\rho} - c_1'' np\epsilon^2\right\} \xrightarrow{p \rightarrow \infty} 0 \\
\mathbb{E}_{\Theta_n \cap \mathcal{U}_M^c}(1 - \Phi) &\leq E_{\Theta_n \cap \mathcal{U}_{M,1}^c}(1 - \Phi) \leq K'' \exp\{-c_2' np\epsilon^2\}
\end{aligned}$$

To verify (c), $\Pi(\Theta_n^c) \leq \Pi(\Theta_{\alpha,n}^c) + \sum_{i=1}^n \Pi(\Theta_{\eta,i,n}^c) + \sum_{k=1}^q \Pi(\Theta_{\zeta,k,n}^c)$. Theorem 5 in Ghosal and Roy (2006) ensures that $\Pi(\Theta_{\eta,i,n}^c) \leq K_3 e^{-c_3(np)^2}$, $\Pi(\Theta_{\zeta,k,n}^c) \leq K_3 e^{-c_3(np)^2}$, Lemma 4 in

Kang et al. (2018) ensures that $\Pi(\Theta_{\alpha,n}^c) \leq K_\alpha e^{-c_\alpha np}$. Hence

$$\begin{aligned}\Pi(\Theta_n^c) &\leq K_\alpha e^{-c_\alpha np} + K_3 e^{-(c_3(np)^2 - \log(n+q))} \\ &\leq K_2 e^{-c_2 np}\end{aligned}$$

□

The proof for Theorem 1 is complete. Note that this can be easily extended to the marginal consistency of α alone by conditioning on other parameters at the true value.

A.3 Proof of Theorem 2

Similar to Theorem 1, we verify the conditions in Theorem A.1 in Choudhuri et al. (2004).

Let θ_0 denote the set of true parameters $\{\beta_0, \gamma_0, \boldsymbol{\xi}_0\}$ that generate the outcome variable Y_i given \mathcal{M}_i, X_i and \mathbf{C}_i . Let $\theta = (\beta, \gamma, \boldsymbol{\xi}) \in \Theta_\beta \times \mathbb{R}^{q+1}$ denote any parameter in the parameter space, where Θ_β is defined in Definition 4.

Lemma 4. (*Prior positivity condition*) Under model (1), define $\Lambda_i(\theta_0, \theta) = \log \{\pi(Y_i; \theta_0)/\pi(Y_i; \theta)\}$, there exists a set $B \subset \Theta$ such that $\Pi(B) > 0$ and for any $\theta \in B$:

$$(a) \liminf_{n \rightarrow \infty} \Pi[\theta \in B : n^{-1} \sum_{i=1}^n \mathbb{E}_{\theta_0} \{\Lambda_i(\theta_0, \theta)\} < \epsilon] > 0 \text{ for any } \epsilon > 0$$

$$(b) n^{-2} \sum_{i=1}^n \text{Var}_{\theta_0} \{\Lambda_i(\theta_0, \theta)\} \rightarrow 0$$

Proof. For one individual i , the density

$$\pi_i(Y_i, \mathcal{M}_i, X_i, \mathbf{C}_i; \theta) = \pi_i(Y_i | \mathcal{M}_i, X_i, \mathbf{C}_i; \theta) \pi_i(\mathcal{M}_i, X_i, \mathbf{C}_i).$$

Here, with the abbreviated notation $\tilde{\boldsymbol{\gamma}} = (\gamma, \boldsymbol{\xi}^\top)^\top \in \mathbb{R}^{q+1}$, and $\tilde{\mathbf{X}}_i = (X_i, \mathbf{C}_i^\top)^\top \in \mathbb{R}^{q+1}$. Hence given $\{\tilde{\mathbf{X}}_i\}_{i=1}^n$ and $\{\mathcal{M}_i(\Delta s_j)\}_{i=1, j=1}^{n, p}$, and denote $\boldsymbol{\mathcal{M}}_i = \{\mathcal{M}_i(\Delta s_j)\}_{j=1}^p$,

$$Y_i \stackrel{\text{ind}}{\sim} N \left(\sum_{j=1}^p \beta(s_j) \mathcal{M}_i(\Delta s_j) + \tilde{\boldsymbol{\gamma}}^\top \tilde{\mathbf{X}}_i, \sigma_Y^2 \right).$$

Given the true parameters $\beta_0(s), \tilde{\boldsymbol{\gamma}}_0$, define the subset

$$B_\delta = \left\{ \Theta : \sup_j |\beta(s_j) - \beta_0(s_j)|^2 \leq \delta, \|\tilde{\boldsymbol{\gamma}} - \tilde{\boldsymbol{\gamma}}_0\|_2^2 \leq \delta \right\}$$

If we denote the mean of Y_i under true parameters as $\mu_{i,0}$, otherwise as μ_i , the log-likelihood ratio for $\theta_0 = (\beta_0(s), \tilde{\gamma}_0)$ versus $\theta = (\beta(s), \tilde{\gamma})$ can be written as

$$\begin{aligned}\Lambda_i(D_{n,i}; \theta_0, \theta) &= \log \{\pi_i(Y_i; \beta_0(s), \tilde{\gamma}_0)\} - \log \{\pi_i(Y_i; \beta(s), \tilde{\gamma})\} \\ &= -\frac{1}{2\sigma_Y^2}(Y_i - \mu_{i,0})^2 + \frac{1}{2\sigma_Y^2}(Y_i - \mu_i)^2\end{aligned}$$

Hence,

$$\begin{aligned}K_{i,n}(\theta_0, \theta) &:= \mathbb{E}_{\theta_0}(\Lambda_i(D_{n,i}; \theta_0, \theta)) = \mathbb{E} \left\{ \mathbb{E}_{\theta_0} \left(\Lambda_i | \mathcal{M}_i, \tilde{\mathbf{X}}_i \right) \right\} \\ &= \mathbb{E} \left\{ \frac{1}{2\sigma_Y^2} (\mu_i - \mu_{i,0})^2 \right\} \\ &\leq \mathbb{E} \left[\frac{1}{2\sigma_Y^2} \left\{ (\tilde{\gamma} - \tilde{\gamma}_0)^T \tilde{\mathbf{X}}_i + \sum_{j=1}^p (\beta(s_j) - \beta_0(s_j)) \mathcal{M}_i(\Delta s_j) \right\}^2 \right]\end{aligned}$$

Note that by equation (4), given $\tilde{\mathbf{X}}_i$, $\mathcal{M}_i(\Delta s_j) \sim N(\mu_i(s_j)\lambda(\Delta s_j), \sigma_M^2\lambda(\Delta s_j))$ with its second moment as $\sigma_M^2\lambda(\Delta s_j) - (\mu_i(s_j)\lambda(\Delta s_j))^2$. When $\lambda(\Delta s_j) = 1/p$, the second moment is $\sigma_M^2/p - (\mu_i(s_j))^2/p^2$, and its 4th moment is of the order $O(p^{-4})$. Hence $\mathbb{E} \left\{ \|\mathcal{M}_i\|_2^2 | \tilde{\mathbf{X}}_i \right\}$ can be upper bounded by a constant, and so does $\text{Var} \left\{ \|\mathcal{M}_i\|_2^2 | \tilde{\mathbf{X}}_i \right\}$. For the finite dimensional vector $\tilde{\mathbf{X}}_i$ with finite 4-th moment (Assumption 2(a)), there is a finite bound $\mathbb{E}\|\tilde{\mathbf{X}}_i\|_2^2 < K_0$.

For any $(\tilde{\gamma}, \beta(s)) \in B_\delta$,

$$K_{i,n}(\theta_0, \theta) \leq \frac{1}{2\sigma_Y^2} \mathbb{E} \left\{ \delta \|\tilde{\mathbf{X}}_i\|_2^2 \|\mathcal{M}_i\|_2^2 \right\}$$

Hence we have $K_{i,n}(\theta_0, \theta) \leq \delta K'$ for some constant $K' > 0$. Similarly, denote $Z_i =$

$(Y_i - \mu_{i,0})/\sigma_Y$ as the standard normal variable under H_0 ,

$$\begin{aligned}
V_{i,n}(\theta_0, \theta) &= \text{Var} \left\{ \mathbb{E}_{\theta_0}(\Lambda_i \mid \tilde{\mathbf{X}}_i, \mathcal{M}_i) \right\} + \mathbb{E} \left\{ \text{Var}_{\theta_0}(\Lambda_i \mid \tilde{\mathbf{X}}_i, \mathcal{M}_i) \right\} \\
\text{Var} \left\{ \mathbb{E}_{\theta_0}(\Lambda_i \mid \tilde{\mathbf{X}}_i, \mathcal{M}_i) \right\} &= \text{Var} \left\{ \frac{1}{2\sigma_Y^2} (\mu_i - \mu_{i,0})^2 \right\} \\
&\leq \frac{1}{4\sigma_Y^4} \text{Var} \left[\left\{ (\tilde{\gamma} - \tilde{\gamma}_0)^\top \tilde{\mathbf{X}}_i + \sum_{j=1}^p (\beta(s_j) - \beta_0(s_j)) \mathcal{M}_i(\Delta s_j) \right\}^2 \right] \\
&\leq \frac{1}{\sigma_Y^4} \text{Var} \left[\delta \|\tilde{\mathbf{X}}_i\|_2^2 + \delta \|\mathcal{M}_i\|_2^2 \right] \\
&\leq \frac{1}{\sigma_Y^4} \text{Var} \left\{ \delta \|\tilde{\mathbf{X}}_i\|_2^2 + \mathbb{E} \left(\delta \|\mathcal{M}_i\|_2^2 \mid \tilde{\mathbf{X}}_i \right) \right\} + \\
&\quad \frac{1}{\sigma_Y^4} \mathbb{E} \left\{ \text{Var} \left(\delta \|\tilde{\mathbf{X}}_i\|_2^2 + \delta \|\mathcal{M}_i\|_{2,p}^2 \mid \tilde{\mathbf{X}}_i \right) \right\} \\
&< \infty
\end{aligned}$$

For the second term,

$$\begin{aligned}
\mathbb{E}_{\theta_0} \left\{ \text{Var}_{\theta_0}(\Lambda_i \mid \tilde{\mathbf{X}}_i, \mathcal{M}_i) \right\} &= \mathbb{E} \left[\text{Var}_{\theta_0} \left\{ -\frac{1}{2} Z_i^2 + \frac{1}{2} \left(Z_i + \frac{\mu_{i,0} - \mu_i}{\sigma_Y} \right)^2 \mid \tilde{\mathbf{X}}_i, \mathcal{M}_i \right\} \right] \\
&= \mathbb{E} \left[\text{Var}_{\theta_0} \left\{ \frac{\mu_{i,0} - \mu_i}{\sigma_Y} Z_i \mid \tilde{\mathbf{X}}_i, \mathcal{M}_i \right\} \right] \\
&= \mathbb{E} \left\{ \frac{1}{\sigma_Y^2} (\mu_i - \mu_{i,0})^2 \right\} \\
&\leq \frac{1}{\sigma_Y^2} \mathbb{E} \left(\delta \|\tilde{\mathbf{X}}_i\|_2^2 + \delta \|\mathcal{M}_i\|_2^2 \right) < \infty
\end{aligned}$$

Hence for any $\beta \in B_\delta$,

$$\frac{1}{n^2} \sum_{i=1}^n V_{n,i}(\beta_0, \beta) \rightarrow 0$$

For any $0 < \epsilon < \delta K'$,

$$\begin{aligned}
&\Pi \left((\beta, \tilde{\gamma}, \sigma_Y) \in B_\delta : \frac{1}{n} \sum_{i=1}^n K_{n,i} < \epsilon \right) \\
&\geq \Pi \left(\sup_j |\beta_0(s_j) - \beta(s_j)| < \sqrt{\epsilon/K'}, \|\tilde{\gamma} - \tilde{\gamma}_0\|_2^2 < \epsilon/K' \right) > 0.
\end{aligned}$$

The last inequality follows from Theorem 1 in [Kang et al. \(2018\)](#) and the assumption that for any $\epsilon > 0$, $\Pi(\|\tilde{\gamma} - \tilde{\gamma}_0\|_2^2 < \epsilon) > 0$.

□

Verifying the Existence of test condition

To verify the existence of test condition, we need the basis expansion expression of model (1). Recall model (1), we abbreviate the scalar and vector covariates and denote $\tilde{\gamma} = (\gamma, \boldsymbol{\xi}^T)^T \in \mathbb{R}^{q+1}$, $\tilde{\mathbf{X}}_i = (X_i, \mathbf{C}_i^T)^T \in \mathbb{R}^{q+1}$. Let $\tilde{\mathcal{M}}_{i,l} = \sum_{j=1}^p \psi_l(s_j) \mathcal{M}_i(\Delta s_j)$, and define the $n \times L_n$ matrix $\tilde{\mathcal{M}}_n := (\tilde{\mathcal{M}}_{i,l})_{i=1, \dots, n, l=1, \dots, L_n}$.

$$\begin{aligned}
Y_i &= \sum_{j=1}^p \beta(s_j) \mathcal{M}_i(\Delta s_j) + \tilde{\gamma}^T \tilde{\mathbf{X}}_i + \epsilon_i \\
&= \sum_{j=1}^p \left\{ \sum_{l=1}^{\infty} \theta_{\beta,l} \psi_l(s_j) \right\} \mathcal{M}_i(\Delta s_j) + \tilde{\gamma}^T \tilde{\mathbf{X}}_i + \epsilon_i \\
&= \sum_{l=1}^{\infty} \theta_{\beta,l} \sum_{j=1}^p \psi_l(s_j) \mathcal{M}_i(\Delta s_j) + \tilde{\gamma}^T \tilde{\mathbf{X}}_i + \epsilon_i \\
&= \sum_{l=1}^{\infty} \theta_{\beta,l} \tilde{\mathcal{M}}_{i,l} + \tilde{\gamma}^T \tilde{\mathbf{X}}_i + \epsilon_i \\
&= (\tilde{\mathcal{M}}_n, \tilde{\mathbf{X}}_n) \begin{pmatrix} \boldsymbol{\theta}_{\beta} \\ \tilde{\gamma} \end{pmatrix} + r_{L_n,i} + \epsilon_i
\end{aligned} \tag{12}$$

The remainder term $r_{L_n,i} = \sum_{l=L_n}^{\infty} \theta_{\beta,l} \sum_{j=1}^p \psi_l(s_j) \mathcal{M}_i(\Delta s_j)$.

Before verifying the existence of test condition, we introduce the following lemma

Lemma 5. *Let independent residual terms*

$$r_{L_n,i} = \sum_{l=L_n}^{\infty} \theta_{\beta,l} \sum_{j=1}^p \psi_l(s_j) \mathcal{M}_i(\Delta s_j)$$

as defined in (12) across $i = 1, \dots, n$. Denote the event $A_{L_n} = [|r_{L_n,i}| < t]$. Then for any given i , and for some sufficiently large positive constant t , $\mathbb{P}[A_{L_n} i.o.] = 1$.

Proof. Denote the mean function in (4) of $\mathcal{M}_i(\Delta s_j)$ as $\mu_i(s_j)$. Then $\mathcal{M}_i(\Delta s_j) = p^{-1} \mu_i(s_j) + p^{-1/2} Z_{i,j}$ where $Z_{i,j}$ is independent standard normal variable across $i = 1, \dots, n, j = 1, \dots, p$. Let $\tilde{\mathcal{M}}_{i,l} = \sum_{j=1}^p \mathcal{M}_i(\Delta s_j) \psi_l(s_j)$. Then

$$r_{L_n,i} = \sum_{l=L_n}^{\infty} \theta_{\beta,l} \tilde{\mathcal{M}}_{i,l} = \sum_{l=L_n}^{\infty} \theta_{\beta,l} \frac{1}{p} \sum_{j=1}^p \mu_i(s_j) \psi_l(s_j) + \sum_{l=L_n}^{\infty} \theta_{\beta,l} \frac{1}{\sqrt{p}} \sum_{j=1}^p \psi_l(s_j) Z_{i,j}$$

which implies that $r_{L_n, i}$ follows a normal distribution with mean

$$\mu_{L_n, i, r} = \sum_{l=L_n}^{\infty} \theta_{\beta, l} \frac{1}{p} \sum_{j=1}^p \mu_i(s_j) \psi_l(s_j)$$

and variance

$$\sigma_{L_n, r}^2 = \frac{1}{p} \sum_{j=1}^p \left(\sum_{l=L_n}^{\infty} \theta_{\beta, l} \psi_l(s_j) \right)^2.$$

Let $\theta_{M, i, l} = p^{-1} \sum_{j=1}^p \mu_i(s_j) \psi_l(s_j)$. Since $\sum_{l=L_n}^{\infty} \theta_{M, i, l}^2 \rightarrow 0$ for any i , and $\sum_{l=L_n}^{\infty} \theta_{\beta, l}^2 \rightarrow 0$ as $L_n \rightarrow \infty$, the mean $\mu_{L_n, i, r} \rightarrow 0$ as $n \rightarrow \infty$.

Given the orthonormality of the basis, and denote $\beta_{L_n}(s) = \sum_{l=1}^{L_n} \theta_{\beta, l} \psi_l(s)$ as the finite basis smooth approximation of $\beta(s)$, write

$$\sigma_{L_n, r}^2 = \int_{\mathcal{S}} |\beta(s) - \beta_{L_n}(s)|^2 d\lambda(s) + r_p = \sum_{l=L_n}^{\infty} \theta_{\beta, l}^2 + r_p,$$

where the approximation error $r_p = \left| \int_{\mathcal{S}} |\beta(s) - \beta_{L_n}(s)|^2 d\lambda(s) - p^{-1} \sum_{j=1}^p |\beta(s_j) - \beta_{L_n}(s_j)|^2 \right|$. From Definition 4(d) $r_p < K_{\beta} p^{-2/d}$, where $K_{\beta} > 0$ is a constant. Hence $\sigma_{L_n, r}^2 \rightarrow 0$ as $n \rightarrow \infty$.

For large enough n , $\mu_{L_n, i, r}$ is bounded for all i . By the normal tail bound (Proposition 2.1.2 in Vershynin (2018)), for $Z \sim N(0, 1)$, $\mathbb{P}(Z > t) \leq \frac{1}{t\sqrt{2\pi}} \exp\{-t^2/2\}$. Then we have

$$\mathbb{P}(r_{L_n, i} > t) \leq \frac{\sigma_{L_n, r}}{t - \mu_{L_n, i, r}} \exp\left\{-\frac{(t - \mu_{L_n, i, r})^2}{2\sigma_{L_n, r}^2}\right\} \leq a_n = C\sigma_{L_n, r} \exp(-c'/\sigma_{L_n, r}^2). \quad (13)$$

By Definition 4, $a_n \leq \exp(-c'n^{\nu_1\nu_2}) < n^{-1}$, hence $\sum_{i=1}^n \mathbb{P}(r_{L_n, i} > t) < \infty$.

$$\mathbb{P}(A_{L_n}^c) = \mathbb{P}(|r_{L_n, i}| > t) \leq \mathbb{P}(r_{L_n, i} > t) + \mathbb{P}(r_{L_n, i} < -t)$$

For the $\mathbb{P}(r_{L_n, i} < -t)$ part, we only need to replace $t - \mu_{L_n, i, r}$ by $t + \mu_{L_n, i, r}$ in (13), and the same conclusion follows, $\sum_{i=1}^n \mathbb{P}(r_{L_n, i} < -t) < \infty$. By Borel-Cantelli Lemma, we can draw the conclusion. □

Lemma 6. (Existence of tests) *There exist test functions Φ_n , subsets $\mathcal{U}_n, \Theta_n \subset \Theta$, and constant $K_1, K_2, c_1, c_2 > 0$ such that*

$$(a) \mathbb{E}_{\theta_0} \Phi_n \rightarrow 0;$$

$$(b) \sup_{\theta \in \mathcal{U}_n^c \cap \Theta_n} \mathbb{E}_\theta(1 - \Phi_n) \leq K_1 e^{-c_1 n};$$

$$(c) \Pi(\Theta_n^c) \leq K_2 e^{-c_2 n}.$$

Proof. To verify the existence of tests, we define the sieve space of β as

$$\Theta_{p,n} := \left\{ \beta \in \Theta_\beta : \sup_{s \in \mathcal{R}_1 \cup \mathcal{R}_{-1}} \|D^\omega \beta(s)\|_\infty < p^{1/(2d)}, \|\omega\|_1 \leq \rho \right\}$$

The construction of the test follows a similar idea as in Lemma 1 in [Armagan et al. \(2013\)](#). For any $\epsilon > 0$, denote

$$\mathcal{U}^c = \{\beta \in \Theta_\beta, \tilde{\gamma} \in \Theta_{\tilde{\gamma}} : \|\beta - \beta_0\|_{2,p} + \|\tilde{\gamma} - \tilde{\gamma}_0\|_2 > \epsilon\}.$$

Following the notations and new formulation of model (1) in (12) under the basis decomposition, we create the test as follows. Denote $\boldsymbol{\theta}_\beta = (\theta_{\beta,1}, \dots, \theta_{\beta,L_n})^\top$, $\boldsymbol{\theta}_w = (\boldsymbol{\theta}_\beta^\top, \tilde{\boldsymbol{\gamma}}^\top)^\top$ as the vector of parameters.

For any $\epsilon > 0$, to test the hypothesis

$$H_0 : \{\beta(s), \tilde{\gamma}\} = \{\beta_0(s), \tilde{\gamma}_0\}, \quad \text{v.s.} \quad H_1 : \{\beta(s), \tilde{\gamma}\} \in \mathcal{U}^c.$$

Define test function

$$\Phi_n = I \left\{ \left\| \left(\tilde{\mathbf{W}}_n^\top \tilde{\mathbf{W}}_n \right)^{-1} \tilde{\mathbf{W}}_n^\top \mathbf{Y} - \boldsymbol{\theta}_w^0 \right\|_2 > \frac{\epsilon}{2} \right\},$$

where $\mathbf{Y} = (Y_1, \dots, Y_n)^\top \in \mathbb{R}^n$. Let $\mathbf{Z} \sim N(0, I_n)$ be a standard normal vector. As defined in the main text above Assumption 3, $\tilde{\mathbf{W}}_n = (\tilde{\mathcal{M}}_n, \tilde{\mathbf{X}}) \in \mathbb{R}^{n \times (L_n + 1 + q)}$, and $\boldsymbol{\theta}_w^0$ denotes the true value of $\boldsymbol{\theta}_w$.

Let $\mathbf{R}_n = (r_{L_n,1}, \dots, r_{L_n,n})^\top \in \mathbb{R}^n$ be the remainder term. Then under H_0 ,

$$\left(\mathbf{Y} - \tilde{\mathbf{W}}_n \boldsymbol{\theta}_w^0 \right) = \mathbf{R}_n^0 + \mathbf{Z} \sigma_Y.$$

Let $H := \left(\tilde{\mathbf{W}}_n^\top \tilde{\mathbf{W}}_n \right)^{-1} \tilde{\mathbf{W}}_n^\top$.

$$H\mathbf{Y} - \boldsymbol{\theta}_w^0 = H \left(\mathbf{Y} - \tilde{\mathbf{W}}_n \boldsymbol{\theta}_w^0 \right) + H \tilde{\mathbf{W}}_n \boldsymbol{\theta}_w^0 - \boldsymbol{\theta}_w^0 = H \left(\mathbf{Y} - \tilde{\mathbf{W}}_n \boldsymbol{\theta}_w^0 \right)$$

Denote the singular value decomposition of $\tilde{\mathbf{W}}_n$ as $\tilde{\mathbf{W}}_n = U\Lambda V^\top$ where $UU^\top = I_n$, $VV^\top = I_{L_n}$, Λ is at most rank L_n , and the smallest singular value is $\sigma_{\min,n}$. Let $\sigma_{\min,n} :=$

$\sigma_{\min}(\tilde{\mathbf{W}})$. For some positive constant c_{\min} , denote event

$$\Sigma = [\sigma_{\min,n} > c_{\min}\sqrt{n}].$$

Let $\chi^2(a, b)$ denote the non-central χ^2 distribution with non-central parameter a and degree b . Then under event Σ ,

$$\begin{aligned} & \left\| H \left(\mathbf{Y} - \tilde{\mathbf{W}}_n \boldsymbol{\theta}_w^0 \right) \right\|_2^2 = \left\| H \left(\mathbf{R}_n^0 + \mathbf{Z} \sigma_Y \right) \right\|_2^2 \\ & = \left(\mathbf{R}_n^0 + \mathbf{Z} \sigma_Y \right)^\top U \Lambda^{-2} U^\top \left(\mathbf{R}_n^0 + \mathbf{Z} \sigma_Y \right) \\ & \leq \left(\mathbf{R}_n^0 + \mathbf{Z} \sigma_Y \right)^\top \sigma_{\min,n}^{-2} \begin{pmatrix} I_{L_n} & 0 \\ 0 & 0_{n-L_n} \end{pmatrix} \left(\mathbf{R}_n^0 + \mathbf{Z} \sigma_Y \right) \\ & = \sigma_Y^2 \sigma_{\min,n}^{-2} \left(\mathbf{R}_n^0 / \sigma_Y + \mathbf{Z} \right)^\top \begin{pmatrix} I_{L_n} & 0 \\ 0 & 0_{n-L_n} \end{pmatrix} \left(\mathbf{R}_n^0 / \sigma_Y + \mathbf{Z} \right) \sim \sigma_Y^2 \sigma_{\min,n}^{-2} \chi^2(L_n, u_n) \end{aligned}$$

$u_n = \frac{1}{\sigma_Y^2} \left\| \begin{pmatrix} I_{L_n} & 0 \\ 0 & 0_{n-L_n} \end{pmatrix} \mathbf{R}_n^0 \right\|_2^2$ is the non-central parameter in the non-central χ^2 distribution of order L_n . Each element in \mathbf{R}_n^0 is the residual term $r_{L_n,i}$.

Several results are available for the upper bound of noncentral χ^2 tail probability, here we use Theorem 7 in [Zhang and Zhou \(2020\)](#), when $x > L_n + 2u_{n,\sigma_Y}$, for some constant c ,

$$\mathbb{P} \left\{ \chi^2(L_n, u_n) - (L_n + u_n) > x \right\} < \exp(-cx)$$

Hence if $\epsilon^2 / (4\sigma_Y^2) \sigma_{\min,n} > L_n + 2u_{n,\sigma_Y}$,

$$\begin{aligned} \mathbb{E}_{\theta_0} \{ \Phi_n I(\Sigma) \} & \leq \mathbb{P} \left\{ \sigma_Y^2 \sigma_{\min,n}^{-2} \chi^2(L_n, u_{n,\sigma_Y}) > \frac{\epsilon^2}{4} \right\} = \mathbb{P} \left\{ \chi^2(L_n, u_{n,\sigma_Y}) > \frac{\epsilon^2}{4\sigma_Y^2} \sigma_{\min,n}^2 \right\} \\ & \leq \exp \left\{ -c \left(\frac{\epsilon^2}{4\sigma_Y^2} \sigma_{\min,n}^2 - L_n - u_{n,\sigma_Y} \right) \right\}. \end{aligned}$$

By Lemma 5, for sufficiently large n , $|r_{L_n,i}| < c_0$ with probability 1. Note that $L_n + u_{n,\sigma_Y} < (1 + c_0^2/\sigma_Y^2) L_n$, given $\sigma_{\min,n} > \sqrt{n}c_{\min} > 0$, for sufficiently large n , there exists a constant $c' > 0$ such that $\epsilon^2 / (4\sigma_Y^2) \sigma_{\min,n}^2 - L_n - u_{n,\sigma_Y} > c'n$. Hence by Assumption 3, $\mathbb{E}_{\beta_0} \{ \Phi_n I(\Sigma) \} \leq \exp\{-c'n\}$ and $\mathbb{E}_{\beta_0}(\Phi) = \mathbb{E}_{\beta_0} \{ \Phi I(\Sigma) \} + \mathbb{E}_{\beta_0} \{ \Phi I(\Sigma^c) \} \leq \exp\{-c'n\} + \exp\{-\tilde{c}n\} \leq \exp\{-\tilde{c}'n\}$, for $n > 2 \log(2)/\tilde{c}'$, where $\tilde{c}' = \min\{\tilde{c}, c'\}/2$.

To find the upper bound of the Type II error, let $\tilde{r}_p = \int_{\mathcal{S}} \{\beta(s) - \beta_0(s)\}^2 \lambda(ds) - \|\beta(s) -$

$\beta_0(s)\|_{2,p}^2$ and $r_{L_n} = \sum_{l=L_n}^{\infty} \theta_{\beta,l}^2$. Then $\tilde{r}_p \rightarrow 0$ as $p \rightarrow \infty$ and $r_{L_n} \rightarrow 0$ as $n \rightarrow \infty$. Note that

$$\int_{\mathcal{S}} \{\beta(s) - \beta_0(s)\}^2 \lambda(ds) = \int_{\mathcal{S}} \left\{ \sum_{l=1}^{\infty} (\theta_{\beta,l} - \theta_{\beta^0,l}) \psi_l(s) \right\}^2 \lambda(ds) = \|\boldsymbol{\theta}_{\beta} - \boldsymbol{\theta}_{\beta^0}\|_2^2 + r_{L_n},$$

where $\boldsymbol{\theta}_{\beta}, \boldsymbol{\theta}_{\beta^0} \in \mathbb{R}^{L_n}$. By $\|\boldsymbol{\theta}_w - \boldsymbol{\theta}_w^0\|_2^2 = \|\boldsymbol{\theta}_{\beta} - \boldsymbol{\theta}_{\beta^0}\|_2^2 + \|\tilde{\gamma} - \tilde{\gamma}_0\|_2^2$,

$$\|\beta(s) - \beta_0(s)\|_{2,p}^2 + \|\tilde{\gamma} - \tilde{\gamma}_0\|_2^2 = \|\boldsymbol{\theta}_w - \boldsymbol{\theta}_w^0\|_2^2 - \tilde{r}_p + r_{L_n}.$$

For a sufficiently large n and p , we have $\tilde{r}_p < \epsilon^2/16$ and $r_{L_n} < \epsilon^2/16$. Then $r_{L_n} - \tilde{r}_p < \epsilon^2/8$. Thus, when $\|\beta(s) - \beta_0(s)\|_{2,p}^2 + \|\tilde{\gamma} - \tilde{\gamma}_0\|_2^2 > \epsilon^2/2$, $\|\boldsymbol{\theta}_w - \boldsymbol{\theta}_w^0\|_2^2 > 3\epsilon^2/8$.

Recall

$$\mathcal{U}^c = \{\beta \in \Theta_{\beta}, \tilde{\gamma} \in \Theta_{\tilde{\gamma}} : \|\beta - \beta_0\|_p + \|\tilde{\gamma} - \tilde{\gamma}_0\|_2 > \epsilon\}.$$

Define the sieve space $\Theta_n := \Theta_{p,n} \times \Theta_{\tilde{\gamma}}$.

$$\begin{aligned} \sup_{\mathcal{U}^c \cap \Theta_n} \mathbb{E}_{\beta}(1 - \Phi_n)I(\Sigma) &= \sup_{\mathcal{U}^c \cap \Theta_n} \mathbb{P} \left\{ \|HY - \boldsymbol{\theta}_w^0\|_2 \leq \frac{\epsilon}{2} \right\} \\ &\leq \sup_{\mathcal{U}^c \cap \Theta_n} \mathbb{P} \left\{ \left| \|HY - \boldsymbol{\theta}_w\|_2 - \|\boldsymbol{\theta}_w - \boldsymbol{\theta}_w^0\|_2 \right| \leq \frac{\epsilon}{2} \right\} \\ &\leq \sup_{\mathcal{U}^c \cap \Theta_n} \mathbb{P} \left\{ \|HY - \boldsymbol{\theta}_w\|_2 > -\frac{\epsilon}{2} + \|\boldsymbol{\theta}_w - \boldsymbol{\theta}_w^0\|_2 \right\} \\ &\leq \sup_{\mathcal{U}^c \cap \Theta_n} \mathbb{P} \left\{ \|HY - \boldsymbol{\theta}_w\|_2 > c_1 \epsilon \right\}, \end{aligned}$$

where $c_1 = \left(\sqrt{3/8} - 1/2\right)$.

Lastly, by Lemma 4 in Kang et al. (2018), for some constant c_2 , $\Pi(\Theta_n^c) \leq K_2' e^{-c_2 p^{1/d}} \leq K_2 e^{-c_2 n}$ with Assumption 1(b) that $p \geq O(n^{\tau d})$. \square

A.4 Proof of Theorem 3

Proof. First we show that, conditioning on all other parameters, the joint posterior of $\alpha(s)$ and $\beta(s)$ can be factored into the marginal posteriors of $\alpha(s)$ and $\beta(s)$. Let $\mathbf{D} =$

$\{\mathbf{Y}, \mathbf{M}, \mathbf{X}, \mathbf{C}\}$. For simplicity, we omit “(s)” in $\alpha(s)$ and $\beta(s)$ in the following derivation.

$$\begin{aligned}
\Pi(\alpha, \beta \mid \mathbf{D}) &= \frac{\Pi(\mathbf{D} \mid \alpha, \beta)\pi(\alpha, \beta)}{\Pi(\mathbf{D})} \\
&= \frac{\Pi(\mathbf{M}, \mathbf{Y} \mid \alpha, \beta, \mathbf{X}, \mathbf{C})\pi(\alpha)\pi(\beta)\pi(\mathbf{X}, \mathbf{C})}{\Pi(\mathbf{Y} \mid \mathbf{M}, \mathbf{X}, \mathbf{C})\Pi(\mathbf{M} \mid \mathbf{X}, \mathbf{C})\pi(\mathbf{X}, \mathbf{C})} \\
&= \frac{\Pi(\mathbf{Y} \mid \mathbf{M}, \alpha, \beta, \mathbf{X}, \mathbf{C})\Pi(\mathbf{M} \mid \alpha, \beta, \mathbf{X}, \mathbf{C})\pi(\alpha)\pi(\beta)}{\Pi(\mathbf{Y} \mid \mathbf{M}, \mathbf{X}, \mathbf{C})\Pi(\mathbf{M} \mid \mathbf{X}, \mathbf{C})} \\
&= \frac{\Pi(\mathbf{Y} \mid \mathbf{M}, \beta, \mathbf{X}, \mathbf{C})\pi(\beta)}{\Pi(\mathbf{Y} \mid \mathbf{M}, \mathbf{X}, \mathbf{C})} \frac{\Pi(\mathbf{M} \mid \alpha, \mathbf{X}, \mathbf{C})\pi(\alpha)}{\Pi(\mathbf{M} \mid \mathbf{X}, \mathbf{C})} \\
&= \Pi(\beta \mid \mathbf{D})\Pi(\alpha \mid \mathbf{D})
\end{aligned}$$

Now,

$$\begin{aligned}
&\Pi(\|\alpha\beta - \alpha_0\beta_0\|_{1,p} > \epsilon \mid \mathbf{D}) \\
&= \Pi(\|(\beta - \beta_0)(\alpha - \alpha_0) + \alpha_0(\beta - \beta_0) + \beta_0(\alpha - \alpha_0)\|_{1,p} > \epsilon \mid \mathbf{D}) \\
&\leq \Pi(\|(\beta - \beta_0)(\alpha - \alpha_0)\|_{1,p} + \|\alpha_0(\beta - \beta_0)\|_{1,p} + \|\beta_0(\alpha - \alpha_0)\|_{1,p} > \epsilon \mid \mathbf{D}) \\
&\leq \Pi(\|(\beta - \beta_0)(\alpha - \alpha_0)\|_{1,p} > \epsilon \mid \mathbf{D}) + \Pi(\|\beta_0(\alpha - \alpha_0)\|_{1,p} > \epsilon \mid \mathbf{D}) + \\
&\quad \Pi(\|\alpha_0(\beta - \beta_0)\|_{1,p} > \epsilon \mid \mathbf{D})
\end{aligned} \tag{14}$$

Given that both α_0 and β_0 are defined on a compact set $\mathcal{S} \in \mathbb{R}^d$ (Definition 4), there exists $K > 0$ such that $\|\alpha_0\|_\infty \leq K$ and $\|\beta_0\|_\infty \leq K$, by Theorem 1, 2, and the norm inequality $\|\cdot\|_{1,p} \leq \|\cdot\|_{2,p}$, the last two terms in (14) goes to 0 in $P_{\alpha_0, \beta_0}^{(n)}$ -probability as $n \rightarrow \infty$.

For any $\delta > 0$,

$$\begin{aligned}
&\Pi(\|(\beta - \beta_0)(\alpha - \alpha_0)\|_{1,p} > \epsilon \mid \mathbf{D}) \\
&\leq \Pi(\|\beta - \beta_0\|_{2,p}\|\alpha - \alpha_0\|_{2,p} > \epsilon \mid \mathbf{D}) \\
&\leq \Pi(\|\beta - \beta_0\|_{2,p}\|\alpha - \alpha_0\|_{2,p} > \epsilon \mid \mathbf{D}, \|\alpha - \alpha_0\|_{2,p} > \delta) \Pi(\|\alpha - \alpha_0\|_{2,p} > \delta \mid \mathbf{D}) + \\
&\quad \Pi(\|\beta - \beta_0\|_{2,p}\|\alpha - \alpha_0\|_{2,p} > \epsilon \mid \mathbf{D}, \|\alpha - \alpha_0\|_{2,p} < \delta) \Pi(\|\alpha - \alpha_0\|_{2,p} < \delta \mid \mathbf{D}) \\
&\leq \Pi(\|\alpha - \alpha_0\|_{2,p} > \delta \mid \mathbf{D}) + \Pi(\|\beta - \beta_0\|_{2,p}\delta > \epsilon \mid \mathbf{D}, \|\alpha - \alpha_0\|_{2,p} < \delta) \\
&= \Pi(\|\alpha - \alpha_0\|_{2,p} > \delta \mid \mathbf{D}) + \Pi(\|\beta - \beta_0\|_{2,p}\delta > \epsilon \mid \mathbf{D}).
\end{aligned}$$

As $n \rightarrow \infty$, $\Pi(\|\alpha - \alpha_0\|_{2,p} > \delta \mid \mathbf{D}) \rightarrow 0$ and $\Pi(\|\beta - \beta_0\|_{2,p}\delta > \epsilon \mid \mathbf{D}) \rightarrow 0$ in $P_{\alpha_0, \beta_0}^{(n)}$ -probability, which implies that $\Pi(\|(\beta - \beta_0)(\alpha - \alpha_0)\|_{1,p} > \epsilon \mid \mathbf{D}) \rightarrow 0$

□

A.5 Proof of Corollary 2

Proof. The proof of the sign consistency is similar to Theorem 3 in Kang et al. (2018).

To show Corollary 2, for simplicity, denote $\mathcal{E}(s) := \alpha(s)\beta(s)$ and $\mathcal{E}_0(s) := \alpha_0(s)\beta_0(s)$, $\forall s \in \mathcal{S}$ as the true function of the total effect. Since both $\alpha(s)$ and $\beta(s)$ satisfy Definition 3, we use the notations

$$\mathcal{R}_i^f := \left\{ s \in \mathcal{S} : \text{sgn}\{f(s)\} = i \right\}, \quad f \in \{\alpha, \beta\}, \quad i \in \{-1, 0, 1\},$$

and by Definition 3, $\mathcal{R}_{\pm 1}^\alpha, \mathcal{R}_{\pm 1}^\beta$ are open sets. Define $\mathcal{R}_1^\mathcal{E} = \left(\mathcal{R}_1^\alpha \cap \mathcal{R}_1^\beta \right) \cup \left(\mathcal{R}_{-1}^\alpha \cap \mathcal{R}_{-1}^\beta \right)$, $\mathcal{R}_{-1}^\mathcal{E} = \left(\mathcal{R}_{-1}^\alpha \cap \mathcal{R}_1^\beta \right) \cup \left(\mathcal{R}_1^\alpha \cap \mathcal{R}_{-1}^\beta \right)$, $\mathcal{R}_0^\mathcal{E} = \mathcal{S} - (\mathcal{R}_1^\mathcal{E} \cup \mathcal{R}_{-1}^\mathcal{E})$, $\mathcal{R}_{\pm 1}^\mathcal{E}$ are open sets. To show $\mathcal{R}_0^\mathcal{E}$ has nonempty interior, if we denote $\bar{A} := \mathcal{S} - A$ as the complementary set of A in \mathcal{S} , we only need to show

$$\left(\overline{\mathcal{R}_1^\alpha \cup \mathcal{R}_{-1}^\alpha} \right) \cup \left(\overline{\mathcal{R}_1^\beta \cup \mathcal{R}_{-1}^\beta} \right) \subseteq \mathcal{R}_0^\mathcal{E}$$

where the LHS has nonempty interior by the Definition 3. $\mathcal{R}_0^\mathcal{E} = \overline{\mathcal{R}_1^\mathcal{E}} \cap \overline{\mathcal{R}_{-1}^\mathcal{E}}$,

$$\begin{aligned} \overline{\mathcal{R}_1^\mathcal{E}} &= \overline{\left(\mathcal{R}_1^\alpha \cap \mathcal{R}_1^\beta \right) \cup \left(\mathcal{R}_{-1}^\alpha \cap \mathcal{R}_{-1}^\beta \right)} \\ &= \left(\overline{\mathcal{R}_1^\alpha \cup \mathcal{R}_{-1}^\alpha} \right) \cup \left(\overline{\mathcal{R}_1^\beta \cup \mathcal{R}_{-1}^\beta} \right) \cup \left(\overline{\mathcal{R}_1^\beta \cup \mathcal{R}_{-1}^\alpha} \right) \cup \left(\overline{\mathcal{R}_1^\alpha \cup \mathcal{R}_{-1}^\beta} \right) \end{aligned}$$

Similarly we can show $\left(\overline{\mathcal{R}_1^\alpha \cup \mathcal{R}_{-1}^\alpha} \right) \cup \left(\overline{\mathcal{R}_1^\beta \cup \mathcal{R}_{-1}^\beta} \right) \subseteq \overline{\mathcal{R}_{-1}^\mathcal{E}}$, hence $\mathcal{R}_0^\mathcal{E}$ has nonempty interior. The parameter space of \mathcal{E} , $\Theta_\mathcal{E}$ satisfies Definition 3.

Now denote $\mathcal{S}_0 = \{s \in \mathcal{S} : \mathcal{E}_0(s) = 0\}$, $\mathcal{S}_+ = \{s \in \mathcal{S} : \mathcal{E}_0(s) > 0\}$, $\mathcal{S}_- = \{s \in \mathcal{S} : \mathcal{E}_0(s) < 0\}$. Notice that $\mathcal{R}_{\pm 1}^{\mathcal{E}_0} \subseteq \mathcal{S}_\pm$, and $\mathcal{S}_0 \subseteq \mathcal{R}_0^{\mathcal{E}_0}$. The key difference is that $\mathcal{S}_{0,\pm}$ are not necessarily open sets.

For any $\mathcal{A} \subseteq \mathcal{S}$ and any integer $m \geq 1$, let Q_p be the discrete measure that assigns $1/p$ mass to each fixed design points in $\{s_j\}_{j=1}^p$, define

$$\mathcal{F}_m(\mathcal{A}) := \left\{ \mathcal{E} \in \Theta_\mathcal{E} : \int_{\mathcal{A}} |\mathcal{E}(s) - \mathcal{E}_0(s)| dQ_p(s) < \frac{1}{m} \right\}.$$

Note that for any $\mathcal{A} \subseteq \mathcal{B} \subseteq \mathcal{S}$, we have $\mathcal{F}_m(\mathcal{S}) \subseteq \mathcal{F}_m(\mathcal{B}) \subseteq \mathcal{F}_m(\mathcal{A})$.

$$\Pi(\mathcal{F}_m(\mathcal{S}_0) \mid \mathbf{D}) \geq \Pi(\mathcal{F}_m(\mathcal{S}) \mid \mathbf{D}) \rightarrow 1, \quad \text{as } n \rightarrow \infty.$$

By the monotone continuity of probability measure,

$$\Pi\{\mathcal{E}(s) = \mathcal{E}_0(s) = 0 \mid \mathbf{D}\} = \Pi\{\mathcal{E}(s) = 0, s \in \mathcal{S}_0 \mid \mathbf{D}\} = \lim_{m \rightarrow \infty} \Pi\{\mathcal{F}_m(\mathcal{S}_0) \mid \mathbf{s}\} = 1, \text{ as } n \rightarrow \infty.$$

Now to show the consistency of the positive sign, for any small $\delta > 0$, denote $\mathcal{S}_+^\delta := \{s \in \mathcal{S} : \mathcal{E}_0(s) > \delta\}$. Because \mathcal{E}_0 is a continuous function, its preimage $\mathcal{E}^{-1}((\delta, \infty))$ supported on \mathbb{R}^d is also an open set, $\mathcal{S}_+^\delta = \mathcal{R}_1^\mathcal{E} \cap \mathcal{E}^{-1}((\delta, \infty))$ hence is also an open set.

For any $s_0 \in \mathcal{S}_+^\delta$, we can find a small open ball $B(s_0, r_1) = \{s : \|s - s_0\|_2 < r_1\} \subseteq \mathcal{S}_+^\delta$. By the continuity of \mathcal{E} and \mathcal{E}_0 , for any large m , there exists $r_2 > 0$ such that $\|s - s_0\|_2 < r_2$ implies $|\mathcal{E}(s) - \mathcal{E}(s_0)| < 1/m$. Let $r = \min\{r_1, r_2\}$.

For any open subset B in \mathcal{S} , Definition 4(d) implies that for any large m , there exists N_m such that for any $n > N_m$,

$$\left| \int_B |\mathcal{E} - \mathcal{E}_0| Q_p(ds) - \int_B |\mathcal{E} - \mathcal{E}_0| \lambda(ds) \right| < \frac{V_m}{2m},$$

where we denote $V_m = \lambda\{B(s_0, r)\} \rightarrow 0$ as $m \rightarrow \infty$.

Hence for any small $\delta > 0$, notice that

$$\begin{aligned} & \frac{1}{V_m} \int_{B(s_0, r)} |\mathcal{E}(s) - \mathcal{E}_0(s)| \lambda(ds) < \frac{1}{m} \\ \Rightarrow & \frac{1}{V_m} \int_{B(s_0, r)} \mathcal{E}(s) \lambda(ds) > \frac{1}{V_m} \int_{B(s_0, r)} \mathcal{E}_0(s) \lambda(ds) - \frac{1}{m} \\ \Rightarrow & \frac{1}{V_m} \int_{B(s_0, r)} \mathcal{E}(s) \lambda(ds) > \delta - \frac{1}{m} \\ \Rightarrow & \exists s_1 \in B(s_0, r), \text{ s.t. } \mathcal{E}(s_1) > \delta - \frac{1}{m} \\ \Rightarrow & \mathcal{E}(s_0) + \frac{1}{m} > \delta - \frac{1}{m}, \forall s_0 \in \mathcal{S}_+^\delta. \end{aligned}$$

Hence we have

$$\begin{aligned} & \Pi\{\forall s_0 \in \mathcal{S}_+^\delta, \mathcal{E}(s_0) > 0 \mid \mathbf{D}\} \geq \Pi\{\forall s_0 \in \mathcal{S}_+^\delta, \mathcal{E}(s_0) \geq \delta \mid \mathbf{D}\} \\ = & \lim_{m \rightarrow \infty} \Pi\left\{\forall s_0 \in \mathcal{S}_+^\delta, \mathcal{E}(s_0) > \delta - \frac{2}{m} \mid \mathbf{D}\right\} \\ \geq & \lim_{m \rightarrow \infty} \Pi\left\{\int_{B(s_0, r)} |\mathcal{E}(s) - \mathcal{E}(s_0)| \lambda(ds) < \frac{V_m}{m} \mid \mathbf{D}\right\} \\ \geq & \lim_{m \rightarrow \infty} \Pi\left\{\int_{B(s_0, r)} |\mathcal{E}(s) - \mathcal{E}(s_0)| dQ_p(s) < \frac{V_m}{2m} \mid \mathbf{D}\right\} = 1, \end{aligned}$$

The proof for the consistency of the negative sign is similar to the positive sign. □

B Example for Assumption 3

In this section, we give an example that demonstrates the generative model (2) satisfies Assumption 3 under some stronger assumptions.

Assumption 4. *When viewing the mediator model (2) as the true generative model of $\tilde{\mathbf{W}}_n$, assume*

1. for any $s \in \mathcal{S}$, $\sum_{i=1}^n X_{i \in M, i}(s) = 0$ and $\sum_{i=1}^n C_{k, i \in M, i}(s) = 0$, $k = 1, \dots, q$, with probability one;
2. for the chosen basis $\{\psi_l(s)\}_{l=1}^\infty$, the individual effects $\eta_i(s)$ can be viewed as one realization of the random Gaussian process $\eta_i \sim \mathcal{GP}(0, \sigma_\eta \kappa)$, and can be decomposed as $\eta_i(s) = \sum_{l=1}^\infty \theta_{\eta, i, l} \psi_l(s)$ where $\theta_{\eta, i, l} \stackrel{ind}{\sim} N(0, \sigma_\eta^2 \lambda_l)$;

Proposition 2. *Under Assumption 4, the least singular value of $\tilde{\mathbf{W}}_n$ satisfies*

$$0 < c_{\min} < \liminf_{n \rightarrow \infty} \sigma_{\min}(\tilde{\mathbf{W}}_n) / \sqrt{n}$$

with probability $1 - \exp(-\tilde{c}n)$ for some constant $\tilde{c}, c_{\min} > 0$.

Recall the notations in (12), $\tilde{\mathbf{W}}_n = (\tilde{\mathcal{M}}_n, \tilde{\mathbf{X}}) \in \mathbb{R}^{n \times (L_n + 1 + q)}$, and $\tilde{\mathbf{X}}_i = (X_i, \mathbf{C}_i^T)^T \in \mathbb{R}^{q+2}$.

The proof of Proposition 2 needs to show that the least singular value of $\tilde{\mathbf{W}}_n$, denoted as $\sigma_{\min}(\tilde{\mathbf{W}}_n)$ satisfies that

$$\mathbb{P}\left(\sigma_{\min}(\tilde{\mathbf{W}}_n) < c\sqrt{n} \mid \mathbf{X}, \mathbf{C}\right) \leq e^{-c'n}$$

Proof. Given (4) for $\mathcal{M}(\Delta s)$ and $\lambda(\Delta s_j) = \frac{1}{p}$, we can write

$$\tilde{\mathcal{M}}_{i, l} = \tilde{\theta}_{\alpha, l} X_i + \sum_{k=1}^q \tilde{\theta}_{\zeta, k, l} C_{i, k} + \theta_{\eta, i, l} + \tilde{\varepsilon}_{i, l}$$

where $\tilde{\varepsilon}_{i, l} \sim N\{0, (\sigma_M^2/p) \sum_{j=1}^p \psi_l(s_j)^2\}$, and each $\tilde{\theta}_{\alpha, l} = \langle \alpha, \psi_l \rangle_p$, $\tilde{\theta}_{\zeta, k, l} = \langle \zeta_k, \psi_l \rangle_p$. Hence we can write

$$\tilde{\mathcal{M}}_n = \tilde{\mathbf{X}} \boldsymbol{\theta}_M + \boldsymbol{\Theta}_E$$

Here, $\boldsymbol{\theta}_M = \begin{pmatrix} \tilde{\theta}_{\alpha,1}, \dots, \tilde{\theta}_{\alpha,L_n} \\ \tilde{\theta}_{\zeta_1,1}, \dots, \tilde{\theta}_{\zeta_1,L_n} \\ \dots \\ \tilde{\theta}_{\zeta_q,1}, \dots, \tilde{\theta}_{\zeta_q,L_n} \end{pmatrix} \in \mathbb{R}^{(q+1) \times L_n}$, $(\boldsymbol{\Theta}_E)_{i,l} = \langle \eta_i, \psi_l \rangle_p + \tilde{\varepsilon}_{i,l}$.

By Assumption 2(c) and Assumption 4.1, we have that $\boldsymbol{\Theta}_E^T \tilde{\mathbf{X}} = \mathbf{0}$. Denote $\mathbf{A}_n = \tilde{\mathbf{X}}^T \tilde{\mathbf{X}}$, then

$$\begin{aligned} \tilde{\mathbf{W}}_n^T \tilde{\mathbf{W}}_n &= \begin{pmatrix} \tilde{\mathcal{M}}_n^T \tilde{\mathcal{M}}_n & \tilde{\mathcal{M}}_n^T \tilde{\mathbf{X}} \\ \tilde{\mathbf{X}}^T \tilde{\mathcal{M}}_n & \tilde{\mathbf{X}}^T \tilde{\mathbf{X}} \end{pmatrix} = \begin{pmatrix} (\tilde{\mathbf{X}} \boldsymbol{\theta}_M + \boldsymbol{\Theta}_E)^T (\tilde{\mathbf{X}} \boldsymbol{\theta}_M + \boldsymbol{\Theta}_E) & (\tilde{\mathbf{X}} \boldsymbol{\theta}_M + \boldsymbol{\Theta}_E)^T \tilde{\mathbf{X}} \\ \tilde{\mathbf{X}}^T (\tilde{\mathbf{X}} \boldsymbol{\theta}_M + \boldsymbol{\Theta}_E) & \tilde{\mathbf{X}}^T \tilde{\mathbf{X}} \end{pmatrix} \\ &= \begin{pmatrix} \boldsymbol{\theta}_M^T \mathbf{A}_n \boldsymbol{\theta}_M + \boldsymbol{\Theta}_E^T \boldsymbol{\Theta}_E & \boldsymbol{\theta}_M^T \mathbf{A}_n \\ \mathbf{A}_n \boldsymbol{\theta}_M & \mathbf{A}_n \end{pmatrix}. \end{aligned}$$

Furthermore,

$$\left(\tilde{\mathbf{W}}_n^T \tilde{\mathbf{W}}_n \right)^{-1} = \begin{pmatrix} (\boldsymbol{\Theta}_E^T \boldsymbol{\Theta}_E)^{-1} & -(\boldsymbol{\Theta}_E^T \boldsymbol{\Theta}_E)^{-1} \boldsymbol{\theta}_M^T \\ -\boldsymbol{\theta}_M (\boldsymbol{\Theta}_E^T \boldsymbol{\Theta}_E)^{-1} & \mathbf{A}_n^{-1} + \boldsymbol{\theta}_M (\boldsymbol{\Theta}_E^T \boldsymbol{\Theta}_E)^{-1} \boldsymbol{\theta}_M^T \end{pmatrix}.$$

This implies that the Schur complement of \mathbf{A}_n in $\left(\tilde{\mathbf{W}}_n^T \tilde{\mathbf{W}}_n \right)^{-1}$ is $(\boldsymbol{\Theta}_E^T \boldsymbol{\Theta}_E)^{-1}$. Denote $\|\cdot\|$ as the operator norm. Notice that $\frac{1}{\sigma_{\min}^2(\tilde{\mathbf{W}}_n)} = \|\tilde{\mathbf{W}}_n^{-1}\|^2 = \left\| \left(\tilde{\mathbf{W}}_n^T \tilde{\mathbf{W}}_n \right)^{-1} \right\|$. By Lemma 7, $\sigma_{\min}(\boldsymbol{\Theta}_E)$ has a lower bound $c\sqrt{n}$ with probability $1 - e^{-c'n}$.

$$\begin{aligned} \left\| \left(\tilde{\mathbf{W}}_n^T \tilde{\mathbf{W}}_n \right)^{-1} \right\|^2 &\leq \left\| (\boldsymbol{\Theta}_E^T \boldsymbol{\Theta}_E)^{-1} \right\|^2 + 2 \left\| (\boldsymbol{\Theta}_E^T \boldsymbol{\Theta}_E)^{-1} \boldsymbol{\theta}_M^T \right\|^2 + \left\| \mathbf{A}_n^{-1} + \boldsymbol{\theta}_M (\boldsymbol{\Theta}_E^T \boldsymbol{\Theta}_E)^{-1} \boldsymbol{\theta}_M^T \right\|^2 \\ &\leq \frac{1}{\sigma_{\min}^4(\boldsymbol{\Theta}_E)} (1 + \|\boldsymbol{\theta}_M\|^2)^2 + \|\mathbf{A}_n^{-1}\|^2 \end{aligned}$$

Note that $\sum_{l=1}^{\infty} \theta_{\alpha,l}^2 < \infty$ and $\sum_{l=1}^{\infty} \theta_{\zeta_k,l}^2 < \infty$, $k = 1, \dots, q$, hence $\|\boldsymbol{\theta}_M\|$ is bounded by a constant. With Assumption 2.(a), $\sigma_{\min}(\mathbf{A}_n) > n$. Hence with probability $1 - e^{-c'n}$,

$$\frac{1}{\sigma_{\min}^4(\tilde{\mathbf{W}}_n)} \leq C \frac{1}{\sigma_{\min}^4(\boldsymbol{\Theta}_E)} + \frac{1}{n^2} \leq \frac{C'}{n^2}$$

Hence $\sigma_{\min}(\tilde{\mathbf{W}}_n) > c\sqrt{n}$ with probability $1 - e^{-c'n}$. \square

Lemma 7. Under model (2),

$$\tilde{\mathcal{M}}_n = \tilde{\mathbf{X}} \boldsymbol{\theta}_M + \boldsymbol{\Theta}_E$$

Then under assumptions 1-4, the smallest singular value $\sigma_{\min}(\Theta_E)$ satisfies that, for some $c_1, c_2 > 0$,

$$\mathbb{P} \left\{ \sigma_{\min}(\Theta_E) < c_1 \sqrt{n} \mid \mathbf{X}, \mathbf{C} \right\} \leq e^{-c_2 n} \quad (15)$$

Proof. To show (15), we can write

$$\Theta_E = \tilde{\Theta}_\eta + \tilde{\Theta}_E + \mathbf{R}_p.$$

To unpack each matrix, we give the (i, l) th element in each matrix: $(\tilde{\Theta}_\eta)_{i,l} = \int_{\mathcal{S}} \eta_i(s) \psi_l(s) \lambda(ds)$, $(\tilde{\Theta}_E)_{i,l} \sim N(0, \sigma_M^2 \int_{\mathcal{S}} \psi_l(s)^2 \lambda(ds))$. Note that we view $\eta_i(s)$ as independent copies of Gaussian processes, and by Assumption 4(b), $(\tilde{\Theta}_\eta)_{i,l} \sim N(0, \lambda_l \sigma_\eta^2)$.

The remainder term \mathbf{R}_p is the approximation error between the continuous integrals and their fixed grid approximation. Denote the fixed grid approximations as $(\Theta_\eta^*)_{i,l} = \frac{1}{p} \sum_{j=1}^p \eta_i(s_j) \psi_l(s_j)$, $(\Theta_E^*)_{i,l} \sim N(0, \frac{1}{p} \sum_{j=1}^p \psi_l^2(s_j))$, and $\mathbf{R}_p = \left\{ \Theta_\eta^* - \tilde{\Theta}_\eta \right\} + \left\{ \Theta_E^* - \tilde{\Theta}_E \right\}$, and $|(\mathbf{R}_p)_{i,l}| \leq K p^{-2/d}$ almost surely for all i, l ,

We need to show

- (i) $\sigma_{\min}(\tilde{\Theta}_E)$ has a lower bound $c\sqrt{n}$ with probability $1 - e^{-\tilde{c}n}$.
- (ii) $\sigma_{\min}(\tilde{\Theta}_E + \tilde{\Theta}_\eta)$ has a lower bound $c\sqrt{n}$ with probability $1 - e^{-\tilde{c}n}$.
- (iii) Adding the error term \mathbf{R}_p does not change this lower bound.

To show (i), let \mathbf{Z} be an $L_n \times n$ dimensional random matrix where the entries are i.i.d standard normal variables. Then by Theorem 1 in Rudelson and Vershynin (2009),

$$\mathbb{P} \left\{ \sigma_{\min}(\mathbf{Z}) < \epsilon \left(\sqrt{n} - \sqrt{L_n - 1} \right) \right\} \leq (C\epsilon)^{n-L_n+1} + e^{-cn}$$

Because we have $L_n = o(n)$ (Assumption 4.3), hence we use a relaxed lower bound, for some $c_0, c'_0 > 0$,

$$\mathbb{P} \left(\sigma_{\min}(\mathbf{Z}) < c_0 \sqrt{n} \right) \leq e^{-c'_0 n}.$$

Because ψ_l forms an orthonormal basis, $\int_{\mathcal{S}} \psi_l^2(s) \lambda(ds) = 1$, $\tilde{\Theta}_E = \sigma_M \mathbf{Z}$.

To show (ii), note $\tilde{\Theta}_\eta = \sigma_\eta \Lambda \mathbf{Z}$. Λ is the diagonal matrix with element λ_l . $\tilde{\Theta}_\eta + \tilde{\Theta}_E = D_E \mathbf{Z}$

where D_E is a diagonal matrix with l th element $\sqrt{\sigma_\eta^2 \lambda_l + \sigma_M^2}$. For any $x \in \mathbb{R}^{L_n}$,

$$\begin{aligned} \sigma_{\min}(D_E Z) &= \min_{\|x\|_2=1} \|Z^T D_E^T x\|_2 = \min_{\|x\|_2=1} \frac{\|Z^T D_E^T x\|_2}{\|D_E^T x\|_2} \|D_E^T x\|_2 \geq \min_{\|y\|_2=1} \|Z^T y\|_2 \min_{\|x\|_2=1} \|D_E^T x\|_2 \\ &= \sigma_{\min}(Z) \sigma_{\min}(D_E) \end{aligned}$$

Hence $\sigma_{\min}(\tilde{\Theta}_\eta + \tilde{\Theta}_E) = \sigma_{\min}(D_E Z) \geq \sigma_{\min}(Z) \sigma_{\min}(D_E) \geq \sqrt{\sigma_\eta^2 \lambda_{L_n} + \sigma_M^2} \sigma_{\min,n}(Z)$. Since $\lambda_{L_n} \rightarrow 0$ as $n \rightarrow \infty$, σ_M^2 is the leading term.

To show (iii), by Weyl's inequality, $\sigma_{\min}(\tilde{\Theta}_\eta + \tilde{\Theta}_E + \mathbf{R}_p) \geq \sigma_{\min}(\tilde{\Theta}_\eta + \tilde{\Theta}_E) - \sigma_{\max}(\mathbf{R}_p)$. Since we have $\max_{i,l} |(\mathbf{R}_p)| \leq K p^{-2/d}$, by Assumption 1 and 4, $\sigma_{\max}(\mathbf{R}_p) \leq K \sqrt{n \times L_n} p^{-2/d} \leq n^{\frac{\nu_1+1}{2}-2\tau} \rightarrow 0$ as $n \rightarrow \infty$ (Assumption 1). \square

C Sensitivity Analysis in Data Application

In this section, we provide details on data preprocessing and selecting the kernel parameters and the prior parameter λ in both models (1) and (2).

To get an appropriate kernel for the real data, we choose the Matérn kernel parameters based on the smoothness of the image mediators. The input images are standardized across subject. To get parameters in the Matérn kernel function as defined in (9), we tune (ρ, u) on a grid in the following way: First, the empirical sample correlations of the image predictors are computed, then the parameters (ρ, u) are obtained using grid search so that the estimated correlation from the kernel function can best align with the empirical correlation computed from the image mediators. The kernel parameters are chosen region-by-region. We refer to this set of kernel parameters as the optimal kernel.

Table 5: Predictive MSE for different kernels

	Optimal Kernel	90% of ρ	$u = 1, \rho = 15$	$u = 0.2, \rho = 80$	110% of ρ
Test MSE	0.515	0.516	0.547	0.539	0.507

To test and compare the performances of different kernels, we split the data into 50% as training data and 50% as testing data. Because the performance of different kernels can be directly compared through testing MSE using the outcome model (1), we conduct a sensitivity analysis using model (1) to select an appropriate set of kernel parameters. The optimal kernel is obtained in the aforementioned way. To test the sensitivity of the kernel, we fix u to be the same as the optimal u , but change ρ to be 90% and 110% of the optimal ρ . Another 2 kernels where u, ρ are constant across different regions are also included in the

comparison. The comparison result is in Table 5. Based on Table 5, the case 110% of the optimal ρ seems to give a slightly better prediction performance, hence we choose this kernel for model (1). The kernel in model (2) remains to be the optimal kernel we choose.

ν	0.01	0.05	0.07	0.1
Training MSE	0.0003	0.3621	0.4043	0.4693
Test MSE	1.8444	0.5079	0.5120	0.5254

Table 6: Training and test MSE for model (1) under different prior thresholding parameter ν for the coefficient $\beta(s)$.

We use the same 2-fold cross validation method to select an appropriate value of ν in the prior of $\beta(s)$. Based on Table 6, if we select a very small $\nu = 0.01$, there is severe overfitting issue; if ν gets too large, the testing accuracy also decreases. Hence based on this 2-fold testing result, $\nu = 0.05$ appears to be the most appropriate thresholding parameter. The running time for fitting model (1) based on 50% of the data is only within 1 hour, so this testing procedure under the current data scale is not very computationally expansive.

Value of ν	0.05	0.08	0.1	0.5
Averaged test MSE	1.008132	1.008075	1.007796	1.007751
Value of ν	1	1.5	1.7	2.0
Averaged test MSE	1.007740	1.007611	1.007532	1.007711

Table 7: Averaged testing MSE over all voxels under different value of ν for model (2).

A similar sensitivity analysis is conducted for model (2) to select ν in the prior of $\alpha(s)$. Estimating the individual effect $\{\eta_i(s)\}_{i=1}^N$ can be very time-consuming, hence the individual effects are set to 0 only for the sensitivity analysis. From table 7, the difference in the testing MSE among different values of ν is very small. Hence we choose $\nu = 0.1$ conservatively to be able to include more activation voxels without compromising the predictive ability.

D Discussion on MALA initial values

As discussed in section 4.3 in the main text, we can use Gibbs sampler to fit the outcome and mediator model first, and then use the posterior mean of β and α as the initial value for MALA algorithm. In the real data analysis, for the mediator model (2), we directly use the posterior mean of θ_α as the initial value for θ_α in the MALA algorithm. For the outcome model (1), we use the Lasso regression to estimate β first, then add ν to locations where

$\beta(s) > 0$, and subtract ν from $\beta(s)$ when $\beta(s) < 0$, to get a hard-thresholded version of the latent GP $\tilde{\beta}$. The last step is to use basis on $\tilde{\beta}$ to get the initial values for θ_β in MALA.